

**Bimodality and Gaps on Globular Cluster Horizontal Branches.
II. The Cases of NGC 6229, NGC 1851 and NGC 2808**

M. Catelan ¹

J. Borissova ²

A. V. Sweigart ¹

and

N. Spassova ²

ABSTRACT

The outer-halo globular cluster NGC 6229 has a peculiar horizontal-branch (HB) morphology, with clear indications of a bimodal HB and a “gap” on the blue HB. In this paper, we present extensive synthetic HB simulations to determine whether peculiar distributions in the underlying physical parameters are needed to explain the observed HB morphology. We find that a unimodal mass distribution along the HB can satisfactorily account for the observed HB bimodality, *provided* the mass dispersion is substantially larger than usually inferred for the Galactic globular clusters. In this case, NGC 6229 should have a well-populated, extended blue tail. A truly bimodal distribution in HB masses can also satisfactorily account for the observed HB morphology, although in this case the existence of an extended blue tail is not necessarily implied. The other two well-known bimodal-HB clusters, NGC 1851 and NGC 2808, are briefly analyzed. While the HB morphology of NGC 1851 can also be reproduced with a unimodal mass distribution assuming a large mass dispersion, the same is not true of NGC 2808, for which a bimodal, and possibly multimodal, mass distribution seems definitely required.

The problem of gaps on the blue HB is also discussed. Applying the standard Hawarden (1971) and Newell (1973) χ^2 test, we find that the NGC 6229 gap is significant at the 99.7% level. However, in a set of 1,000 simulations, blue-HB gaps comparable to the observed one are present in $\sim 6\% - 9\%$ of all cases. We employ a new and simple formalism, based on the binomial distribution, to explain the origin of this discrepancy, and conclude that Hawarden’s method, in general, substantially overestimates the statistical significance of gaps.

¹ NASA/Goddard Space Flight Center, Code 681, Greenbelt, MD 20771, USA

² Institute of Astronomy, Bulgarian Academy of Sciences, 72 Tsarigradsko chaussée, BG – 1784 Sofia, Bulgaria

Subject headings: Stars: Hertzsprung-Russell (HR) diagram — Stars: Horizontal-Branch — Stars: Population II — Globular clusters: individual: NGC 6229, NGC 1851, NGC 2808.

1. Introduction

The outer-halo globular cluster (GC) NGC 6229 (C1645+476) has recently been studied photometrically by Borissova et al. (1997, hereafter Paper I). These authors showed that the horizontal-branch (HB) morphology of this cluster is characterized by two peculiar properties: i) A distinctly bimodal distribution in $B-V$ colors, consistent with the relatively small number of RR Lyrae variables, compared to the blue HB and red HB populations; and ii) At least one “gap” on the blue HB, as previously noted by Carney, Fullton, & Trammell (1991).

Bimodal-HB clusters are relatively rare, as are clusters with gaps on the blue HB. NGC 6229 is one of only two known cases—the other being NGC 2808 (Sosin et al. 1997a)—where these two anomalies are simultaneously present. As argued by many authors, an understanding of the nature of the detected peculiarities in “bimodal” and “gap” clusters would be of paramount importance for understanding the nature of the second parameter phenomenon (e.g., Buonanno, Corsi, & Fusi Pecci 1985; Rood et al. 1993; Stetson, Vandenberg, & Bolte 1996; Paper I).

These considerations have prompted us to perform a theoretical investigation of the problem of HB bimodality and gaps. In particular, we have considered the following questions: i) Can HB bimodality be produced by canonical evolutionary models? ii) If so, what are the requirements for producing HB bimodality in the specific cases of NGC 6229, NGC 1851, and NGC 2808? iii) Are gaps on the blue HB a natural consequence of stellar evolution, as claimed by some authors? iv) What is the statistical significance of gaps?

In this paper, we present extensive synthetic HB simulations for NGC 6229. We begin in the next section by laying out a proposed nomenclature for both defining and differentiating “bimodal” and “gap” clusters. In Sec. 3, we describe the theoretical procedure used in Sec. 4 to compute synthetic HBs for NGC 6229. The statistical significance of gaps on the blue HB is next discussed in Sec. 5. In Sec. 6, we present additional computations for the bimodal-HB clusters NGC 1851 and NGC 2808. In Sec. 7, we discuss some previously proposed scenarios for the origin of HB bimodality and gaps, in the light of the present results. Finally, Sec. 8 summarizes our results. In an Appendix, a compilation is presented and discussed of GCs which may present signs of HB bimodality and gaps, according to the definitions laid out in Sect. 2. Several of these clusters may require more detailed observational and theoretical investigations in the future.

2. Definition of HB Bimodality and Gaps

Before discussing HB bimodality and gaps, it is important to clearly define these terms, since they have been used somewhat ambiguously in the literature. This is especially important for bimodality, because the presence or lack of “bimodality” depends on the quantity being considered. For instance, a cluster may be bimodal in $B-V$, but not in T_{eff} or mass.

The term “bimodal HB” has sometimes been applied to clusters with a gap on the blue HB

(e.g., Crocker, Rood, & O’Connell 1988). More traditionally (e.g., Norris 1981; Lee, Demarque, & Zinn 1988), this term has been used to characterize those clusters having two *main modes* in the $B-V$ color distribution, one on the red HB and one on the blue HB.

We shall call “*bimodal-HB clusters*” those objects which show a dip in the *number counts* at the RR Lyrae level, in comparison with both the blue HB and the red HB. In other words, a bimodal-HB cluster, in this scheme, is one for which $B > V < R$, where B , V , and R are the number of stars on the blue HB, inside the instability strip, and on the red HB, respectively. Such a definition will generally imply that the distribution in $B-V$ colors along the HB has two preferred statistical modes as well—one on the red HB clump, and one on the blue HB.

We emphasize that this definition of HB bimodality does not necessarily imply that *all* quantities characterizing an HB distribution will have two preferred statistical modes. For instance, the distribution in magnitudes may very well have just one mode, as is commonly the case. Most importantly, whether the underlying *temperature* and/or *mass* distributions have two preferred statistical modes as well, as we shall see, can only be determined after a thorough case-by-case study. The main advantage of our definition is that it is based entirely on *directly observed quantities*; its purpose is to serve as a helpful guide when searching for clusters with potentially more than one statistical mode in the underlying physical parameters, especially the temperature and mass. At any rate (see also Rood & Crocker 1985b), our definition of HB bimodality immediately suggests an important difference between the bimodal-HB clusters thus defined and the archetypal “standard” cluster M3 = NGC 5272, for which $B : V : R \simeq 0.33 : 0.41 : 0.26$ (Buonanno et al. 1994).

We shall call “*gap clusters*” those objects which show more or less pronounced gaps along the blue HB, or possibly even on the red HB or *inside* the instability strip. In those instances where a gap *coincides* with the instability strip—as in the case of NGC 2808 (Harris 1974)—we shall call the object a “bimodal-HB cluster,” *not* a “gap cluster.” A bimodal-HB cluster may, however, simultaneously be classified as a gap cluster, provided an additional gap is present somewhere along the blue or red HB. It is interesting to note that only four objects have thus far been simultaneously classified as “bimodal-HB” and “gap” clusters, namely: NGC 2808, NGC 6229, NGC 6388, and NGC 6441.

In the Appendix, we present the results of an extensive survey of GC CMDs which may conform to the above definitions of HB bimodality and gaps. We believe that this compilation and the accompanying discussion will prove useful for future investigations of HB bimodality and gaps.

We shall now proceed to describe in detail our theoretical efforts to model the HB of NGC 6229, beginning with a discussion of the theoretical framework used in our analysis.

3. Theoretical Framework: Evolutionary Tracks and Synthetic HBs

3.1. Stellar Models and HB Simulations

The evolutionary tracks for this project were computed with the same numerical procedures as in Sweigart & Gross (1976, 1978), except for the use of updated input physics as described by Sweigart (1997a, 1997b). A solar-scaled metallicity of $Z = 0.001$ was adopted, as seems appropriate for NGC 6229 ($[\text{Fe}/\text{H}] = -1.44$; Harris 1996), after assuming a slight enhancement of the α -elements (Salaris, Chieffi, & Straniero 1993). The standard value for the main-sequence (MS) helium abundance, as derived for Galactic GCs from the R -method (e.g., Buzzoni et al. 1983), was assumed, i.e., $Y_{\text{MS}} = 0.23$.

An evolutionary track for a mass of $0.82 M_{\odot}$ was first evolved up the red giant branch (RGB) without mass loss and then through the helium flash to the zero-age HB (ZAHB). This choice for the mass corresponds to an age at the tip of the RGB of 15 Gyr. Lower mass ZAHB models were then generated by removing mass from the envelope of this $0.82 M_{\odot}$ ZAHB model. The minimum ZAHB mass was $0.497 M_{\odot}$, which only slightly exceeds the core mass $M_c = 0.4937 M_{\odot}$ for the adopted chemical composition. In total, a grid of 16 HB tracks was computed. This grid was supplemented by two additional HB tracks for $M = 0.495 M_{\odot}$ and $0.496 M_{\odot}$ for producing Fig. 15 only. Some canonical HB tracks for $Y_{\text{MS}} = 0.23$, $Z = 0.0005$ from Sweigart (1997a, 1997b) were also used in preparing Fig. 3.

The above HB evolutionary tracks were fed into an updated version of Catelan’s (1993) HB synthesis code. We refer the reader to this paper for a description of the method. However, several improvements to this code deserve mention.

The prescriptions of Kurucz (1992) have been adopted to transform from the theoretical ($\log L$, $\log T_{\text{eff}}$) to the observational (M_V , $B-V$) plane. Silberman & Smith (1996) have discussed the possible need for a shift of the zero point of the Kurucz bolometric corrections (BCs). No such shift was applied in the present study, since it is unclear that there is a solid physical motivation for applying the same “zero-point” correction to stars of widely different temperatures, gravities and metallicities, and thus of widely different atmospheric structures (but see Buser & Kurucz 1978, especially their Sec. V, for a more detailed discussion of the “arbitrariness” of the zero points of BC scales). Hill’s (1982) Hermite interpolation algorithm has been employed for interpolation with respect to $\log g$ and $\log T_{\text{eff}}$. When necessary, linear interpolation was adopted with respect to $[\text{m}/\text{H}]$.

Random numbers were generated using the procedure described by Wichmann & Hill (1987). For the generation of Gaussian deviates, the Box-Müller method (see description in Bevington & Robinson 1992) has been adopted. This method reliably describes the *tails* of Gaussian distributions, which may be particularly important in the modelling of scarcely populated, extended blue HBs. It is important to bear in mind the subtle, but fundamental, difference between a *Gaussian deviate* and a *Gaussian distribution*. Deviates are randomly-generated distributions which asymptotically approach the true distribution it is meant to represent in the limit $N \rightarrow \infty$. In CMDs of Galactic GCs, the total number of observed HB stars is often

$N_{\text{HB}} \lesssim 200$ (see, e.g., Table 1 in Lee et al. 1994). For samples of this size, one can expect the distinction to become important (see, e.g., Newman, Haynes, & Terzian 1989). In the remainder of this paper, however, the more familiar term “Gaussian distribution” will be used interchangeably with “Gaussian deviate.”

Observational errors in B and V , assumed to be Gaussian, have also been introduced using the Box-Müller method.

The synthetic HB code has also been adapted to generate bimodal distributions in mass. Instead of being characterized by three free parameters, $\langle M_{\text{HB}} \rangle$ (mean mass), σ_M (width of the Gaussian mass distribution) and N_{HB} (total number of HB stars), as in the unimodal case, the bimodal simulation requires *six* free parameters: two $(\langle M_{\text{HB}} \rangle, \sigma_M)$ pairs, N_{HB} , and a normalization factor f_1 that gives the fraction of the N_{HB} stars contributed by the first Gaussian.

The existence of a photometric limit in the CMD below which the incompleteness becomes 100% has been accounted for in the following way. After generating a simulated CMD in the standard way, a search is performed for any stars fainter than $\Delta V_{\text{lim}}^{\text{RR}}$ below the mean RR Lyrae level. Such stars are then discarded, and “replacement” stars are generated from the same original mass distribution. The process is iterated until all N_{HB} stars lie above the brightness limit.

Finally, in the present computations a width $\Delta \log T_{\text{eff}} = 0.075$ has been adopted for the instability strip.

3.2. The ℓ_{HB} Coordinate

A numerical routine has also been added to the HB synthesis code that automatically computes the ℓ_{HB} coordinate, which is linear along the HB ridgeline (Ferraro et al. 1992a, 1992b; Dixon et al. 1996). Coordinates of this type are very useful for studying the presence of gaps on the HB (Crocker et al. 1988; Rood & Crocker 1989), since they effectively remove the degeneracy in HB colors for $(B-V)_0 \lesssim 0$ (cf. Fig. 16 below).

To compute the HB ridgeline, we make use of the synthetic HB code to generate a “fiducial” HB model with 8,000 stars. Mean colors and magnitudes are then computed at selected points along the HB, and a cubic-spline curve fitted to these points. (One ridgeline thus obtained can be seen in Fig. 8a below.)

After projecting each star onto the ridgeline, a length value is then computed along it, from the star’s location up to the red limit of the distribution. The scaling relations $\Delta \ell_{\text{HB}} / \Delta (B-V)_0 \simeq 22.24$ and $\Delta \ell_{\text{HB}} / \Delta M_V \simeq 4.63$ are assumed, which are similar to those obtained by Dixon et al. (1996) for M79 = NGC 1904.

In Fig. 1, we show the HB region of the CMD of NGC 6229, taken from Paper I. Using the above procedure, we obtained the NGC 6229 ℓ_{HB} distribution from these data. A total of

31 RR Lyrae variables was assumed to be present—the maximum number suggested in Paper I—and their colors were assumed to be distributed randomly inside the instability strip boundaries given by Carney et al. (1991). The resulting ℓ_{HB} distribution is shown in Fig. 2. Note that the maximum value attained by ℓ_{HB} corresponds very closely to the L_t value provided by Fusi Pecci et al. (1993) for this cluster, $L_t = 14$.

The bimodal nature of the NGC 6229 CMD is also evident in this plot. One clearly recognizes the red HB “clump” in the $0 \leq \ell_{\text{HB}} \lesssim 3$ region. The blue tail corresponds to the well-populated region at $\ell_{\text{HB}} \gtrsim 7$. In between, one finds a “valley” in the distribution. The gap on the blue HB is easily recognized, lying at $\ell_{\text{HB}} \simeq 8.8$, with width $\Delta\ell_{\text{HB}} \approx 0.5$. We will analyze the statistical significance of this feature in Sec. 5 below.

4. Synthetic HBs for NGC 6229

It has sometimes been suggested that bimodal HBs may be produced by unimodal mass distributions along the HB (Norris 1981; Lee et al. 1988; Walker 1992). In the present section, we will investigate this possibility for the case of NGC 6229 on the basis of detailed HB simulations.

We begin by displaying some key HB morphology parameters for NGC 6229 in Table 1. The number counts have been corrected for completeness as described in Paper I. The following quantities are given: the Mironov (1972) parameter $B/(B + R)$; the Lee-Zinn parameter $(B - R)/(B + V + R)$ (cf. Lee et al. 1994); the Buonanno (1993) parameter $(B2 - R)/(B + V + R)$; the number ratios $B : V : R$, obtained assuming that approximately half of the new candidate RR Lyrae variables (Paper I) are “real;” the total length of the HB L_t (Fusi Pecci et al. 1993), computed as in Sec. 3.2 above; and, finally, the color of the red edge of the HB, HB_{RE} (cf. Fusi Pecci et al. 1993). In the simulations, HB_{RE} was defined as the mean $(B - V)_0$ color for the reddest 2.5% of the HB stars.

Our goal was to select synthetic HBs with unimodal and bimodal mass distributions (UMD and BMD, respectively) that would best match *all* of these HB morphology parameters. We have run several hundred test cases with large ($\sim 500 - 5,000$) populations of HB stars to narrow down the allowed range of free parameters that permit a satisfactory global fit to the observed HB morphology. In the BMD case, the search was further constrained by the (arbitrary) requirement that $\sigma_{M,1} \approx \sigma_{M,2}$. We also assumed that $\Delta V_{\text{lim}}^{\text{RR}} = 2.2$ mag (Paper I).

This search yielded the following two simulations:

$$\begin{aligned} \text{UMD} : \quad & \langle M_{\text{HB}} \rangle = 0.5595 M_{\odot}, \quad \sigma_M = 0.1 M_{\odot}; \\ \text{BMD} : \quad & \langle M_{\text{HB},1} \rangle = 0.59 M_{\odot}, \quad \sigma_{M,1} = 0.025 M_{\odot}, \\ & \langle M_{\text{HB},2} \rangle = 0.67 M_{\odot}, \quad \sigma_{M,2} = 0.025 M_{\odot}, \\ & f_1 = 0.578. \end{aligned}$$

For these two selected cases, we then computed two series of synthetic HBs, each containing 1,000

simulations with $N_{\text{HB}} = 235$ (Paper I) stars. Observational scatter was also added, assuming Gaussian error distributions with $\sigma_V = 0.017$ mag and $\sigma_B = 0.031$ mag, as suggested by the data in Paper I. Variable and non-variable HB stars were treated in exactly the same way, as far as the observational errors are concerned; we thus expect these HB simulations to show significant overlap in color between the variable and non-variable stars. The average values of the HB morphology parameters, as well as the corresponding standard deviations, are given in Table 1 for both the UMD and BMD cases.

Inspection of Table 1 discloses that *both the UMD and BMD cases are quite successful at reproducing, to within the errors, all of the major HB morphology parameters for NGC 6229*. In the UMD case, however, this has required a large value for the HB mass dispersion. Our test runs show that significantly smaller σ_M values (but still larger than the typical values listed, e.g., by Catelan 1993) would still reproduce the observed HB morphology parameters, except for $(B2 - R)/(B + V + R)$, which provides a stringent constraint on the allowed simulations by demanding that a large fraction of the blue HB population lie at $(B - V)_0 < 0.02$ mag. These results indicate that *HB bimodality is consistent with a unimodal distribution in mass, provided the mass dispersion is sufficiently large* (for further discussion see Sec. 7 below).

The size of the mass dispersion required for bimodality is, however, a function of the adopted metallicity. This is shown in Fig. 3, where the run of $V/(B + V + R)$ as a function of σ_M is compared with those of $B/(B + V + R)$ and $R/(B + V + R)$ for two metallicities. In this plot, the Lee-Zinn HB morphology parameter was held fixed at the value appropriate for NGC 6229. The displayed quantities were obtained by averaging over ~ 10 simulations with $N_{\text{HB}} \simeq 1,000$ for each σ_M value. A larger σ_M value is clearly required in the lower Z case to produce HB bimodality (as defined in Sec. 2). This behavior can be straightforwardly understood if we recall that the HB effective temperature becomes less sensitive to changes in mass as the metallicity decreases [see Fig. 7 in Buonanno et al. (1985)].

Fig. 4 shows twelve cases selected at random from the series of 1,000 UMD simulations. The reason for displaying several of these simulations in one single plot is to highlight the effects of the statistical fluctuations upon the HB morphology. We emphasize that all displayed models are based on exactly the same underlying physical assumptions and input parameters. A similar random sample of 12 models for the BMD case is displayed in Fig. 5.

Histograms showing the ℓ_{HB} and $\log T_{\text{eff}}$ distributions for the UMD simulation in Fig. 4b are given in Fig. 6. Fig. 7 shows similar histograms for the BMD simulation in Fig. 5f. (These two examples were chosen randomly from the set of simulations presented in Figs. 4 and 5.) From Fig. 6, one sees that *a bimodality in ℓ_{HB} , or even in $\log T_{\text{eff}}$, does not necessarily imply a true bimodality in the underlying mass distribution*. For a sufficiently wide UMD, one peak in the temperature distribution will naturally occur at the red end of the HB, where the evolutionary tracks for the higher masses tend to pile up. Unless it is erased by statistical fluctuations, a peak on the blue HB will also be naturally present, *provided* the peak of the UMD corresponds to a

ZAHB point on the blue HB.

A quick inspection of Figs. 4 and 5 suggests that it may be difficult to discriminate between the UMD and BMD cases. A closer analysis reveals, however, that the blue HB in the UMD case tends to be more uniformly populated than in the BMD case due to the very large σ_M value required in the UMD case. This effect is indeed suggested in Figs. 6 and 7. In fact, a two-sample Kolmogorov-Smirnov test applied to the 1,000 UMD and 1,000 BMD simulations slightly favors the UMD case, in the mean, as the actual representation of the observed ℓ_{HB} distribution in NGC 6229 (Fig. 2). However, the difference is not very large, and we do not consider it significant for the following reasons: i) The synthetic HBs contain more blue HB stars than does the CMD in Paper I, because the completeness corrections discussed in Paper I have been taken into account in the *number counts* only, and ii) The precise number and color distribution of the RR Lyrae stars in the observed CMD are uncertain.

The remarkable similarity between the UMD and BMD simulations can be largely ascribed to the adopted brightness limit, $\Delta V_{\text{lim}}^{\text{RR}} = 2.2$ mag. In fact, the very large mass dispersion in the UMD case leads to a *very* extended blue tail. This point is illustrated in Fig. 8 by two sample simulations with $N_{\text{HB}} = 300$, computed for the UMD case with $\Delta V_{\text{lim}}^{\text{RR}} \rightarrow \infty$. Mean HB morphology parameters over 12 such simulations are given in Table 2.

As one can see, the distribution may reach as hot as the extreme HB (EHB) region. The ℓ_{HB} and $\log T_{\text{eff}}$ distributions for the simulation in Fig. 8b, plotted in Fig. 9, shows a significant number of EHB stars. However, it is important to note that a lower value for $(B2 - R)/(B + V + R)$ would produce a less extended blue HB tail. In the BMD case, on the other hand, a very extended blue tail is not *necessarily* implied, as shown in Fig. 10, although a long blue tail might also be present in this case, if the mass dispersion for the low-mass mode is larger than assumed here. In fact, as discussed in Paper I, there are some indirect indications that a well-populated blue tail may be present in NGC 6229.

Finally, it is important to note that the horizontal part of the synthetic HBs seems to be quite “flat.” The observations, on the other hand, indicate that the red end of the blue HB may be brighter than the main portion of the red HB (Paper I), as previously suggested by Stetson et al. (1996) for NGC 1851 and NGC 2808. If real, this would imply that, in all likelihood, a different parameter besides the mass varies between the blue and the red HB. One natural candidate is the envelope helium abundance (Sweigart 1997b). *We emphasize the importance of constraints of this type for assessing the cause of HB bimodality on a cluster-by-cluster basis.*

5. On the Reality and Nature of HB Gaps

A particularly important aspect of Figs. 4 and 5 is the surprisingly large fraction of the HB simulations that display prominent gaps. In this section, we will present a new method for analyzing the statistical significance of such gaps. We begin with the standard analysis of the

gap found on the *observed* ℓ_{HB} distribution of NGC 6229. This gap is clearly present in Fig. 2 at $\ell_{\text{HB}} \simeq 8.8$, and has a size $\Delta\ell_{\text{HB}} \simeq 0.5$.

5.1. The Gap on the Observed HB

The standard method for evaluating the statistical significance of gaps on the HB is the one advanced by Hawarden (1971) and used by many other researchers (e.g., Newell 1973; Crocker et al. 1988). The method works in the following way: from the average slope of the cumulative distribution of stars to the blue and to the red of a detected gap, and from its estimated width, one computes the “expected” number of stars inside the gap, N_{\star} . From the number of stars which are *actually* found inside the gap, N_{gap} ($= N_0$ in Hawarden’s notation), the following “ χ^2 statistic” is then formed:

$$\chi^2 = \frac{(N_{\star} - N_{\text{gap}})^2}{N_{\star}}. \quad (1)$$

Standard statistical tables (e.g., Abramowitz & Stegun 1965, Table 26.7) are then used to evaluate the “statistical significance” of the detected feature. Although not explicitly stated, apparently the assumed number of degrees of freedom in Hawarden’s test is $\nu = 1$, for an example is given of a case where $\chi^2 = 8.5$, whose probability of being “an accidental result is about 0.5 per cent.” That applications of the method generally assume $\nu = 1$ is also supported by the values provided by Newell in his Table 1, and by Crocker et al. in their Table 1, although we have been unable to reproduce the probability value in the latter study for NGC 1851.

If we apply the same method to NGC 6229, we find that ≈ 14 HB stars are expected inside the gap region, whereas only ≈ 3 are found (cf. Figs. 1 and 2). Thus, $\chi^2 = 8.64$, which, for $\nu = 1$, would imply a 99.7% probability that the gap is not a statistical fluctuation. How does this compare with the results of the Monte Carlo simulations?

5.2. Gaps on the Synthetic HBs

If the probability that the NGC 6229 gap is not a statistical fluctuation is indeed as high as 99.7%, one would expect only about 3 out of every 1,000 simulations to present a “NGC 6229-like” gap on the blue HB. To test this prediction, we have carefully inspected each of our 1,000 simulations in the $(M_V, B-V)$ plane for the presence of a gap on the blue HB. We find that $\sim 6\% - 9\%$ of all simulations show gaps which are comparable in size and/or sharpness with the observed one. *This stands in sharp contrast with the negligibly small fraction that would be expected on the basis of Hawarden’s (1971) method.* In fact, if gaps which are a little less sharp or narrower are also included, we find that up to $\approx 15\%$ of all simulations show gaps on the blue HB.

These numbers increase further by a few percent if gaps inside the instability strip or on the red HB are also included.

Selected synthetic HBs with quite prominent gaps are shown in Fig. 11 (UMD case) and in Fig. 12 (BMD case). These were chosen from the same two sets of 1,000 simulations previously discussed. As one can see, prominent gaps can indeed appear virtually anywhere along the HB.

These Monte Carlo simulations suggest that Hawarden’s (1971) method substantially overestimates the probability that gaps are “real.” To understand the reason for this, we recall that Hawarden’s method attempts to answer the following question: What is the probability that a gap *at the observed location* is real? By requiring a gap to be at the observed location, this method effectively constrains the probability that a gap can arise from a statistical fluctuation. There is, of course, no way of knowing a priori where a statistical fluctuation might occur. Consequently the more fundamental question to ask is: What is the probability that a gap will be found *somewhere* along the HB? This latter question provides an additional degree of freedom to the statistical analysis and therefore a more realistic estimate of the importance of statistical fluctuations.

The present situation for the HB gaps resembles the controversy that arose some time ago regarding the significance of gaps on the RGB. Sandage, Katem, & Kristian (1968) first reported that a “major significant” gap was present on the RGB of M15, and subsequently similar features were detected in several other GCs. However, Monte Carlo experiments by Bahcall & Yahil (1972) showed that RGB gaps occurred far more frequently than expected from the Sandage et al. statistical arguments. As described by Renzini & Fusi Pecci (1988) some twenty years later, “the tendency (...) has been for such [RGB] gaps to get filled with increasing sample size, as simulations had anticipated (Bahcall & Yahil 1972).” Newman et al. (1989) discuss a similar problem in the study of the periodicities in galaxy redshifts.

5.3. On the Probability of Finding Gaps *Somewhere* along the HB

We consider now a simple mathematical model, based on the binomial distribution, for estimating the probability of finding a gap somewhere along the HB.

Consider a hypothetical GC whose ℓ_{HB} distribution is perfectly uniform. Let us divide the HB into N_{b} bins of identical width $\Delta\ell_{\text{HB}}$. We then place, at random, N_{HB} stars onto the HB of this cluster, and construct an ℓ_{HB} distribution for the stars in this sample. Clearly, the probability that a *given* star will be placed in the j -th bin is $p_j = 1/N_{\text{b}}$, since the distribution is known *a priori* to be uniform. We ask the question: what is the probability P_j that out of this sample of N_{HB} stars the total number of stars N_j in the j -th bin will be less than or equal to some value N_{gap} ? The answer to this question is given by the binomial distribution:

$$P_j = \sum_{k=0}^{N_{\text{gap}}} \binom{N_{\text{HB}}}{k} p_j^k (1 - p_j)^{(N_{\text{HB}} - k)}, \quad (2)$$

where $p_j = p = 1/N_{\text{b}}$.

By applying this simple model to the blue HB of NGC 6229—which is equivalent to assuming, as a first crude approximation, that its “true” underlying ℓ_{HB} distribution is uniform—we can estimate the probability that a gap of the size actually present in NGC 6229 will be seen in the j -th bin. (In fact, we have noted before that the distribution of stars along the blue tail, for a large mass dispersion σ_M , will indeed be quite uniform in the mean.) For NGC 6229, the number of stars on the blue HB (corrected for completeness) is $N_{\text{BHB}} = 147$ (Paper I). Further, the blue HB distribution extends from $\ell_{\text{HB}} \approx 7$ to $\ell_{\text{HB}} \approx 14$. As we have seen, the size of the observed NGC 6229 gap is $\Delta\ell_{\text{HB}} \approx 0.5$, and the number of stars inside the gap is 3. If NGC 6229’s blue-HB ℓ_{HB} distribution is divided into 14 bins of size $\Delta\ell_{\text{HB}} = 0.5$, then the probability that a given star will be found in the j -th bin is $1/14$. We then find from equation (2) that the probability that the j -th bin will contain 3 or less stars is

$$\begin{aligned} P_j &= \sum_{k=0}^3 \binom{147}{k} \left(\frac{1}{14}\right)^k \left(1 - \frac{1}{14}\right)^{(147-k)} \\ &= 0.58\%. \end{aligned} \quad (3)$$

The probability of finding a gap as sharp as, or sharper than, the one found in NGC 6229 *in the j -th bin* is indeed quite low. However, as already anticipated, this calculation does not give an answer to the *really* important question, namely: What is the probability P_{gap} that a sharp gap will be found *somewhere* along the blue HB?

We can apply the above formalism to answer this question. The total number of bins is 14, and, from equation (3), the probability of a gap occurring in the j -th bin is $P_j = 0.0058$. Thus from the binomial distribution the probability that a gap will be found *somewhere* along the blue HB is given by

$$\begin{aligned} P_{\text{gap}} &= \binom{14}{1} 0.0058^1 (1 - 0.0058)^{(14-1)} \\ &= 7.5\%. \end{aligned} \quad (4)$$

Thus, the probability that a gap will be present on the blue HB is *at least an order of magnitude larger than commonly realized* (Hawarden 1971; Newell 1973; Crocker et al. 1988). Although this rough estimate is based on a crude model that can certainly be refined with a more realistic

approximation for the probability function p_j , it is in reasonable agreement with the results of our detailed Monte Carlo experiments.

Does this imply that all the known HB gaps (cf. Sec. 2) are caused by statistical fluctuations? While the probability that a blue HB gap is due to a statistical fluctuation is at least an order of magnitude larger than previously realized, this does not imply that some, and perhaps all, of the detected gaps are not real in some deeper physical sense. This issue can only be settled by a very careful case-by-case study of the available observational data. For instance, the occurrence of gaps at very similar positions on the HB in clusters of nearly identical metallicity might be suggestive of a genuine physical mechanism for producing gaps. Therefore, besides reassessing the statistical significance of each individual gap, it would be very important to apply some of the proposed tests which are capable of constraining their possible physical causes (Rood & Crocker 1985a, 1985b; Crocker et al. 1988; D’Cruz et al. 1996; Sweigart 1997b). We intend to employ both canonical and non-canonical stellar evolution models, coupled with Monte Carlo techniques, in order to attempt to make some progress in this direction (Catelan & Sweigart 1997).

6. Synthetic HBs for NGC 1851 and NGC 2808

We have shown that the UMD simulations can satisfactorily account for the HB bimodality found in NGC 6229, provided the mass distribution is substantially wider than commonly assumed for the GCs. As a further step in this investigation, we now consider whether a similarly wide mass distribution might be responsible for the HB bimodality in the archetypal clusters NGC 1851 and NGC 2808.

6.1. On the HB Bimodality in NGC 1851

Table 3 gives the HB morphology parameters for NGC 1851. These parameters are based on the following number counts derived from Fig. 7 in Walker (1992): $B = 49$, $V = 16$, $R = 96$. We have also used $B2/(B + V + R) = 0.17$ from Buonanno et al. (1997) and the L_t and HB_{RE} values from Fusi Pecci et al. (1993).

We have performed a search for a UMD simulation that would optimally match these HB morphology parameters. A simulation characterized by $\langle M_{HB} \rangle = 0.665 M_{\odot}$, $\sigma_M = 0.055 M_{\odot}$ was found to give a satisfactory fit. We then computed a sequence of 100 simulations with $N_{HB} = 161$, assuming an observational scatter of $\sigma_{B,V} < 0.01$ mag. The resulting mean values for the HB morphology parameters are also given in Table 3. Two representative simulations are shown in Fig. 13. As one can see, the match to the observed HB parameters is quite satisfactory, and we conclude that the HB bimodality of NGC 1851 may also be caused by a unimodal, if peculiarly wide, HB mass distribution. Walker (1992) has noted that the red HB is more sharply peaked in color than would be predicted by simulations similar to those in Fig. 13. However, the HST CMD

for NGC 1851 by Sosin et al. (1997b) seems to show a red HB that resembles more closely the morphology expected from the present simulations.

The observed and expected L_t values in Table 3 seem to differ by a substantial amount—although we cannot guarantee that the two quantities are on exactly the same scale, even though our calibration reproduces the Fusi Pecci et al. (1993) L_t value for NGC 6229 (cf. Sec. 4). The reason for this disagreement can be understood by comparing the two simulations in Fig. 13. In panel a, a simulation with a relatively “short” blue tail is displayed; this is similar to the CMD presented by Walker (1992) in his Fig. 6, as well as the one previously published by Stetson (1981)—the latter having been used by Fusi Pecci et al. in their measurement of L_t . In about 2 out of every 3 UMD simulations, however, we find a dribble of quite hot stars, lying at $M_V > 3$ mag, which increase the predicted value of L_t . A few such hot stars are indeed suggested by the CMDs in Walker’s Fig. 5 (see also Saviane et al. 1997). The *Ultraviolet Imaging Telescope* (Parise et al. 1994; Landsman 1994) did detect two very hot HB stars in NGC 1851, one of which Landsman has confirmed to be a radial velocity cluster member. Additional hot HB stars may be present closer to the center of this very concentrated cluster, where crowding prevented Parise et al. from obtaining reliable UV colors. The present simulations suggest that these stars may be compatible with a standard, if quite wide, UMD.

6.2. On the HB Bimodality in NGC 2808

We have also computed some simulations to see if the HB bimodality in NGC 2808 could also be reproduced with a UMD. We employed the number counts from Sosin et al. (1997a) to estimate the HB morphology parameters for this cluster. Some 800 HB stars were measured in NGC 2808 by these authors using the HST, yielding one of the most spectacular CMDs for a GC ever obtained. The number of RR Lyrae variables in NGC 2808 seems to be very low (Clement & Hazen 1989), although claims have on occasion been raised that the instability strip could be more substantially populated (Byun & Lee 1991). In the HST field, however, the number of RR Lyrae variables seems to be safely constrained to be < 20 , and possibly much lower (Dorman 1997). This gives $V/(B + V + R) = 0.024$ as an upper limit to the fraction of RR Lyrae variables in NGC 2808.

We were totally unable to obtain a satisfactory UMD simulation for NGC 2808. The minimum number of RR Lyrae variables in our simulations occurs when the peak of the mass distribution is placed at $\langle M_{\text{HB}} \rangle \approx 0.497 M_{\odot}$, with an exceedingly large mass dispersion $\sigma_M > 0.3 M_{\odot}$; even in this (probably highly artificial) case, however, the RR Lyrae fraction is as high as $V/(B + V + R) \simeq 0.06$. In fact, in a series of 100 synthetic HBs for these UMD parameters (where observational scatter $\sigma_{B,V} < 0.015$ mag was also added), the minimum RR Lyrae fraction was $V/(B + V + R) = 0.039$. We show the simulation with the minimum number of variables in Fig. 14a, and another simulation with a curious gap on the blue HB in Fig. 14b. The agreement between these simulations and the CMD presented by Sosin et al. (1997a) is not satisfactory. It appears therefore that a bimodal, or possibly multimodal, mass distribution is required to fit the

NGC 2808 HB.

7. Discussion

With the insight provided by our HB simulations, we shall now analyze some previously proposed scenarios for the origin of HB bimodality and gaps. For a discussion of non-standard scenarios, we refer the reader to the recent papers by van den Bergh (1996), Catelan (1997), Sosin et al. (1997a), and Sweigart (1997b).

7.1. HB Bimodality

It has sometimes been suggested that bimodal HBs may be accounted for by unimodal mass distributions along the HB (Norris 1981; Lee et al. 1988; Walker 1992). In particular, Walker has argued that, given a sufficiently wide dispersion in mass along the HB, bimodality is naturally implied. But does this apply equally well to both $B-V$ colors and temperatures?

In Figs. 15a and 15b we show the $(\log L, \log T_{\text{eff}})$ and $(M_V, B-V)$ planes, respectively, for a “reference” synthetic HB populated by a large number (100,000) of HB stars randomly sampled from a uniform distribution in mass along the ZAHB over the range $0.495 \leq M/M_{\odot} \leq 0.820$. This large number of HB stars was used to minimize any statistical fluctuations. Fig. 15b shows that, on the observational diagram, the number of stars at intermediate $B-V$ colors (where the RR Lyrae variables are found) seems to be significantly depleted in comparison with the number of stars both on the blue HB and on the red HB. In Fig. 16, we show the color-temperature relation from the Kurucz (1992) model atmospheres for a representative gravity and metallicity. These diagrams show very clearly the well-known fact (e.g., Rood & Crocker 1989) that bimodal color distributions may be produced due to the piling up of HB evolutionary tracks at the low-temperature (i.e., high-mass) end, and to the insensitivity of the $B-V$ color to temperature changes for $\log T_{\text{eff}} \gtrsim 3.9$. Thus, HB bimodality—at least in the observational sense previously defined—is naturally implied for sufficiently wide mass distributions, as we had indeed found on the basis of detailed simulations. However, inspection of Fig. 15a reveals that, for a uniform mass distribution, a rather uniform distribution in temperatures results.

Interestingly, Walker (1992) has proposed that the morphology of the HB evolutionary tracks—in particular, the presence of long “blue loops” in the post-ZAHB evolution—might produce a bimodal distribution in temperature (and thus also in the number counts and $B-V$ colors) along the HB. The only requirement, according to Walker, is that the mass dispersion be substantially larger than typically assumed in HB simulations. Can track morphology really lead to two main statistical modes in the HB temperature distribution? To address this question, we show in Fig. 17 a synthetic HB employing 20,000 stars randomly sampled from a uniform mass distribution over a mass range chosen to cover the temperature range in Walker’s Fig. 8

for NGC 1851. Our assumption of a flat mass distribution favors Walker’s suggestion by adding more blue HB stars than in the detailed simulations for this cluster shown in Fig. 13. The same chemical composition as in Walker’s study was also adopted. Two histograms for T_{eff} are given in Fig. 17: one which includes the canonical evolution of the HB stars away from the ZAHB, and another where all evolution away from the ZAHB is suppressed. As one can clearly see, both histograms are comprised of a single statistical mode on the red clump region, accompanied by a quite uniformly populated distribution extending to higher temperatures. There is no sign of a peak in the temperature distribution blueward of the instability strip. These histograms clearly show that evolution off the ZAHB does not help in producing two main modes in the temperature distribution.

We have carried out a similar simulation using the HB evolutionary tracks of Lee & Demarque (1990), as shown in Fig. 18. As remarked by Catelan & de Freitas Pacheco (1993), the Lee & Demarque HB evolutionary tracks, for some still unclear reason, present blueward loops which are much longer in $\Delta \log T_{\text{eff}}$ (for the same chemical composition) than in other independent HB evolutionary calculations. This difference in track morphology dramatically affects the synthetic HBs, particularly the luminosity width, as can clearly be seen by comparing Figs. 17 and 18. Interestingly, the more recent Koopmann et al. (1994) and Yi, Lee, & Demarque (1995) HB tracks show blueward loops which are in much better agreement with those presented by, e.g., Sweigart (1987), as well as with those employed in the present work. The differences in track morphology notwithstanding, this simulation also shows a remarkably flat temperature distribution blueward of the instability strip. (The slight irregularities in this HB simulation are due to the coarseness of the Lee & Demarque grid.) The histograms once again demonstrate that the HB evolution does not contribute to the production of two main statistical modes in the temperature distribution. Our results do not therefore support the argument (Lee et al. 1988) that bimodality can arise naturally from “evolution away from the ZAHB.”

There is, however, one circumstance under which the blueward loops may be *directly* responsible for producing HB bimodality. For some combinations of evolutionary parameters—for instance, for large values of the envelope helium abundance, or for low values of the helium-core mass M_c —blueward loops may become *very* long indeed (see, e.g., Sweigart & Gross 1976). Primordial (Shi 1995) or evolutionary (Sweigart 1997a, 1997b) processes might be responsible for a large helium abundance in HB stars. A substantial decrease in M_c would, however, be harder to justify (Sweigart 1994; Catelan, de Freitas Pacheco, & Horvath 1996). In either case, for sufficiently large Y or low M_c values ZAHB stars on the red HB clump will evolve along extremely long blueward loops and thereby produce a substantial number of blue HB stars, and possibly even a relatively long blue tail. Moreover, provided the ZAHB mass distribution does not populate the region between the red clump and the blue HB, few stars would be present near the instability strip, because of the rapid evolutionary pace at these intermediate temperatures. If such a scenario were to be responsible for a bimodal HB, however, we would expect the HB distribution to be *sloped* on the CMD (Catelan & de Freitas Pacheco 1996). Interestingly, bimodal

and sloped HBs have recently been reported for the metal-rich GCs NGC 6388 and NGC 6441 (Piotto et al. 1997; Rich et al. 1997). We have carried out extensive simulations to explore this scenario in detail and have confirmed that high Y values can lead to both bimodal and sloped HBs. Preliminary results for these simulations have been presented by Sweigart & Catelan (1997a) and will be discussed more fully in a future paper (Sweigart & Catelan 1997b).

7.2. Gaps on the Blue HB

The change in the morphology of canonical post-ZAHB evolutionary tracks as a function of mass has sometimes been invoked to explain the presence of blue-HB gaps (e.g., Norris et al. 1981; Lee et al. 1994). In particular, it has been argued that the NGC 288 gap, and possibly the NGC 6752 one, may be easily explained in this way (Lee et al. 1994). However, numerical experiments by Castellani et al. (1995) failed to provide conclusive evidence for or against this suggestion.

Inspection of Figs. 15a and 15b shows no significantly underpopulated regions on the blue HB in either diagram. Similar plots using the Lee & Demarque (1990) HB tracks do not show any significantly underpopulated regions either. This indicates that, contrary to previous claims, *gaps on the blue HB are not caused by the morphology of canonical HB tracks.*

One noteworthy feature in Fig. 15b is the non-monotonic behavior of the number counts as a function of $B-V$ at $B-V \approx 0.2 - 0.3$. No corresponding feature seems to be present in the theoretical plane (cf. Figs. 15a and 17). Inspection of the Kurucz (1992) color transformations (cf. Fig. 16) discloses that this anomaly is related to an abrupt change in slope of the $(B-V) - \log T_{\text{eff}}$ relation at this region. We refer the reader to the papers by Gratton, Carretta, & Castelli (1996, esp. their Sec. 5) and Lejeune, Cuisinier, & Buser (1997) for discussions of this feature, which is not present in their more recent color-temperature transformations.

Some experiments with the non-standard evolutionary tracks of Sweigart (1997a, 1997b) show that track morphology may play a rôle in generating gaps, but only if some physical parameter(s) (such as Y or M_c) changes *abruptly* as a function of temperature along the ZAHB, thus effectively generating a *break* in track morphology at a given temperature, as opposed to the continuous and smooth change that is found in the canonical case (Fig. 15).

A gap on the extreme HB is also predicted by the scenario outlined by D’Cruz et al. (1996). In their framework, very hot extreme HB stars ($\log T_{\text{eff}} \approx 4.5$; cf. their Fig. 2) are produced by the stars which undergo the He flash on the white dwarf cooling curve as a consequence of high mass loss rates on the RGB (Castellani & Castellani 1993). In this case, however, the predicted gap location would be even hotter than the gap in NGC 6752 (Sweigart 1997b).

8. Summary

The following are the main results of the present investigation:

- HB bimodality may be caused by a unimodal distribution in mass, provided the mass dispersion on the HB is substantially larger than in “typical” clusters. In particular, the HB bimodality in NGC 6229 and NGC 1851 is quite satisfactorily accounted for by unimodal mass distributions with mass dispersions $\sigma_M = 0.1 M_\odot$ and $0.055 M_\odot$, respectively. In the NGC 6229 case, however, a unimodal mass distribution would imply the presence of a very extended and well-populated blue tail. Further observations are urgently needed to check whether such an extended HB is present or not. Our results do not support the claim (Lee et al. 1988) that HB bimodality arises from “evolution off the ZAHB;”
- The NGC 2808 HB distribution cannot be reproduced by a unimodal mass distribution, but seems most decidedly to require a bimodal, or possibly multimodal, mass distribution;
- Extensive Monte Carlo simulations show that gaps along the HB are much more likely to occur as a consequence of statistical fluctuations than has been previously realized from the standard Hawarden (1971) and Newell (1973) χ^2 technique. In particular, $\simeq 6\% - 9\%$ of our simulations show blue HB gaps resembling the one observed in NGC 6229. In contrast, the Hawarden-Newell technique predicts a probability of 99.7% that the observed gap in NGC 6229 is real. The reason for this discrepancy can be traced to the fact that the Hawarden-Newell technique requires the statistical fluctuation to produce a gap *at the observed location*. As a result, the Hawarden-Newell method substantially overestimates the probability that a gap is real. The more fundamental question is whether or not statistical fluctuations can produce gaps of the observed size and/or sharpness *somewhere* along the HB. The present investigation, in analogy with a previous study by Bahcall & Yahill (1972) on the significance of gaps on the RGB, thus indicates that a comprehensive reassessment of the significance and nature of gaps on the blue HB is urgently required. In this regard, our study already shows that, contrary to previous claims (e.g., Lee et al. 1994), gaps on the blue HB are *not* caused by the change in shape of the evolutionary tracks as a function of mass;
- We present a new mathematical model, based on the binomial distribution, for estimating the statistical significance of HB gaps and demonstrate that it predicts a probability for the reality of a gap that is consistent with our simulations;
- Refinement of the several possible *observational tests* for the cause of HB bimodality and the presence of gaps along a distribution (e.g., Crocker et al. 1988; Sweigart 1997b), and their careful application to studies of each individual cluster in which an anomaly of this sort has been reported, is thus *strongly encouraged*. Upon this depends the reliable establishment of the nature of the “multiple parameters” that seem to be affecting, to a larger or smaller

extent, the observed HB distributions in Galactic GCs (e.g., Buonanno et al. 1985; Rood & Crocker 1985a, 1985b; Crocker et al. 1988; Rood et al. 1993; Stetson et al. 1996; Sosin et al. 1997a; Fusi Pecci & Bellazzini 1997; Ferraro et al. 1997b; Sweigart 1997b; etc.).

M. C. would like to thank W. V. D. Dixon, B. Dorman and W. B. Landsman for useful information and discussions. This work was performed while M. C. held a National Research Council–NASA/GSFC Research Associateship. A. V. S. acknowledges support through NASA grant NAG5-3028. This research was supported in part by the Bulgarian National Science Foundation grant under contract No. F-604/1996 with the Bulgarian Ministry of Education and Sciences.

Appendix

A Compilation of (Candidate) “Bimodal” and “Gap” GCs

In this Appendix, we present a comprehensive compilation of GCs whose HBs may satisfy the definitions of HB bimodality and gaps laid out in Sect. 2. We hope this will provide a useful guide for future investigations of the problem of HB bimodality and gaps.

A list of clusters that appear to satisfy the definition of HB bimodality presented in Sect. 2 can be found in Table 4. In this table, values for the cluster metallicity $[\text{Fe}/\text{H}] = \log(\text{Fe}/\text{H})_{\text{GC}} - \log(\text{Fe}/\text{H})_{\odot}$ and core concentration c from Harris (1996; values adopted come from the May 1997 issue of his catalogue) are given in the third and fourth columns, respectively. We list the c values for these clusters because of the suggestion that core concentration may be correlated with anomalies in the HB morphology (e.g., Fusi Pecci et al. 1993; Castellani 1994 and references therein). The last column gives the references where attention was drawn to the possible HB bimodality.

With respect to this table, the following additional comments are in order. For NGC 6362, the suggestion of an HB bimodality (Paper I) was based on the Lee, Demarque, & Zinn (1994) number counts, which in turn relied on Alcaino’s (1972) color-magnitude diagram (CMD). This cluster has been more recently observed by Alcaino & Liller (1986), but their CMDs include only a few stars on the HB, so that a definite answer regarding its HB bimodality must await a more extensive investigation. For NGC 6712, the CMD published by Martins & Harvel (1981) may give some support for HB bimodality, although the uncertainties remain large. The Lee et al. number counts for this cluster, based on Sandage & Smith’s (1966) CMD, give $B : V : R = 0.15 : 0.11 : 0.74$. New photometry for NGC 6723 has very recently been presented by Fullton & Carney (1996); their CMD may give some support to the classification of this object as a bimodal-HB cluster. For M75 = NGC 6864, new CCD investigations are especially encouraged, since the latest CMD available (Harris 1975) is strongly suggestive of an NGC 1851-like HB bimodality. Caputo et al. (1973) have also suggested that M72 = NGC 6981 may have a bimodal HB. However, the recent study by Kadla et al. (1995) has identified 9 possible new variable stars in the cluster. If confirmed, this would rule out M72 as a bimodal-HB cluster, since the number ratios would become $B : V : R \simeq 0.33 : 0.34 : 0.33$ (Kadla et al. 1995). Note that we do not classify M5 = NGC 5904 as a bimodal-HB cluster, as opposed to Smith & Norris (1983) and Lee et al. (1988), since the number counts reported by Sandquist et al. (1996) in their Table 7 do not show a dip at the RR Lyrae level—a conclusion independently supported by Markov’s (1997) photometry (but see also Reid 1996).

Another possible case of HB bimodality is provided by the relatively metal-rich GC M69 = NGC 6637. As pointed out by Ferraro et al. (1994; cf. their Sect. 7), a red HB clump seems to be accompanied by what appears to be a quite long blue tail. And yet, no RR Lyrae variables have been reported to be cluster members, according to the latest edition of the Sawyer Hogg

(1973) catalogue on variable stars in GCs (Clement 1996). Likewise, the GC Palomar 2 has been included in Table 4 as yet another example of HB bimodality, since the CMD of Harris et al. (1997a) clearly shows both a red clump and an extended blue tail, but few RR Lyrae variables are known (or suspected) to be present in the cluster (Clement 1996; Harris et al. 1997a).

Gap clusters are listed in Table 5, where the columns have the same meaning as in Table 4.

Racine (1971) lists a few additional candidate gap clusters besides those in Table 5: NGC 4147; M2 = NGC 7089; M12 = NGC 6218; and M22 = NGC 6656. However, the latest published CMDs for most of these clusters (NGC 4147: Aurière & Lauzeral 1991; M2: Aurière & Cordoni 1983, Montgomery 1995; M12: Montgomery 1995, Brocato et al. 1996; M22: Samus et al. 1995) either do not support his suggestion or are not suitable for a reliable confirmation. The presence of a gap on the blue HB of M5 (Brocato, Castellani, & Ripepi 1995) is not clearly supported by the extensive CMD study by Sandquist et al. (1996), although a gap-like feature is also present in Reid’s (1996) photometry (cf. his Fig. 4). Similarly, while according to Ferraro, Fusi Pecci, & Buonanno (1992b) NGC 5897 contains a gap on the blue HB, a similar feature does not seem to be present in the CMD by Sarajedini (1992). The M55 gap noted by Desidera (1996) is not very pronounced, and further analysis of this cluster is encouraged.

Fusi Pecci et al. (1993) report that NGC 1261 and M30 = NGC 7099 have HB gaps (cf. their Table 1). However, Ferraro et al. (1993) have remarked that “the blue HB tail (...) [of NGC 1261] does not show any marked gap or clump,” so we do not classify this object as a gap cluster. With regard to M30, neither the *Hubble Space Telescope* (HST) ultraviolet and visual CMDs published by Yanni et al. (1994) and Mould et al. (1996), nor the ground-based photometry by Montgomery (1995), Bergbusch (1996), or Burgarella & Buat (1996), seem to show HB gaps either. M3 is also included in the Fusi Pecci et al. list of gap clusters. Although this may eventually prove to be the case (see Ferraro et al. 1997a for a detailed discussion), we shall not classify M3 as a gap cluster in the present paper.

The case of NGC 288 deserves special attention, since the classic HB gap reported by Buonanno et al. (1984) and Bergbusch (1993)—a feature which, according to Crocker et al. (1988), has a null probability of being a statistical fluctuation—seems to have completely vanished in the latest, high-quality CCD analysis by Kaluzny (1996), although the latter study shows that a few extremely hot HB stars may be well separated from the main body of the HB. The famous NGC 288 gap is not evident in Bolte’s (1992) study either, although Bergbusch (1993) not only confirms it, but also suggests that an additional “distinct” gap may be present on the blue HB. In the case of ω Cen, the reader may find it instructive to inspect Figs. 12 and 13 in Kaluzny et al. (1996), along with Figs. 8 and 9 in Kaluzny et al. (1997), to evaluate the degree to which the appearance of gap-like features may depend on the specific fields analyzed, sample sizes, quality of the data, and other observational details. Similarly, we draw attention to Figs. 1 and 2 in Kaluzny (1997), where CMDs for NGC 6397 are presented. While a gap is quite evident in his Fig. 1, it is absent in his Fig. 2, where different reduction procedures and data selection and treatment were

adopted. A blue-HB gap was also not found in the previous study of this cluster by Alcaino et al. (1987).

M70 = NGC 6681 is included in Table 5 because the Watson et al. (1994) UV-visible CMD shows a gap (not noted by those authors) at $T_{\text{eff}} \approx 8,700$ K (cf. their Fig. 2). The gap is not clear in the ground-based optical photometry by Brocato et al. (1996), though.

Worth noting is the fact that, in general, gaps have been reported mostly on the blue HB. Fusi Pecci et al. (1992) discuss, however, the possible existence of gaps on the red HB (in particular in the case of M3; see also Renzini & Fusi Pecci 1988), which they argue may represent the progeny of blue straggler stars. As far as we are aware, the NGC 6638 and IC 4499 gaps are the only ones which have been reported to lie *inside* the instability strip, although we note, in passing, that Fig. 10 in Buonanno et al. (1994) for M3 also shows evidence for a similar gap. Of course, the uncertainties involved in the analysis of this kind of gap are very large, since determining equilibrium colors for RR Lyrae variables is a far from trivial task. Reid (1996), for instance, notices that a gap between the RR Lyrae strip and the red HB may or may not exist in M5, depending on which technique one employs.

Analysis of Table 4 discloses that HB bimodality only occurs in intermediate-to-high metallicity GCs. No correlation with central concentration seems to be present. Table 5 fails to reveal any correlation between the presence of HB gaps and either [Fe/H] or core concentration. However, since it seems likely that some of the detected gaps may be due to statistical fluctuations (cf. Sec. 5), any real correlations would tend to be erased by the “noise” introduced by these “spurious” detections.

REFERENCES

- Abramowitz, M., & Stegun, I. A. 1965, Applied Mathematics Series, Vol. 55, Handbook of Mathematical Functions (Washington, D. C.: National Bureau of Standards)
- Alcaino, G. 1972, A&A, 16, 220
- Alcaino, G., Buonanno, R., Caloi, V., Castellani, V., Corsi, C. E., Iannicola, G., & Liller, W. 1987, AJ, 94, 917
- Alcaino, G., & Liller, W. 1986, AJ, 91, 303
- Aurière, M., & Cordoni, J.-P. 1983, A&AS, 51, 135
- Aurière, M., & Lauzeral, C. 1991, A&A, 244, 303
- Bahcall, J. N., & Yahil, A. 1972, ApJ, 177, 647
- Bailyn, C. D., Sarajedini, A., Cohn, H., Lugger, P. M., & Grindlay, J. E. 1992, AJ, 103, 1564
- Battistini, P., Bregoli, G., Fusi Pecci, F., Lolli, M., & Bingham, E. A. E. 1985, A&AS, 61, 487
- Bergbusch, P. A. 1993, AJ, 106, 1025
- Bergbusch, P. A. 1996, AJ, 112, 1061
- Bevington, P. R., & Robinson, D. K. 1992, Data Reduction and Error Analysis for the Physical Sciences, 2nd Edition (New York: McGraw-Hill)
- Bolte, M. 1992, ApJS, 82, 145
- Borissova, J., Catelan, M., Spassova, N., & Sweigart, A. V. 1997, AJ, 113, 692 (Paper I)
- Brocato, E., Buonanno, R., Malakhova, Y., & Piersimoni, A. M. 1996, A&A, 311, 778
- Brocato, E., Castellani, V., & Ripepi, V. 1995, AJ, 109, 1670
- Buonanno, R. 1993, in ASP Conf. Ser. Vol. 48, The Globular Cluster–Galaxy Connection, ed. G. H. Smith & J. P. Brodie (San Francisco: ASP), 131
- Buonanno, R., Caloi, V., Castellani, V., Corsi, C., Ferraro, I., & Piccolo, F. 1988, A&AS, 74, 353
- Buonanno, R., Caloi, V., Castellani, V., Corsi, C., Fusi Pecci, F., & Gratton, R. 1986, A&AS, 66, 79
- Buonanno, R., Corsi, C. E., Bellazzini, M., Ferraro, F. R., & Fusi Pecci, F. 1997, AJ, 113, 706
- Buonanno, R., Corsi, C. E., Buzzoni, A., Cacciari, C., Ferraro, F. R., & Fusi Pecci, F. 1994, A&A, 290, 69
- Buonanno, R., Corsi, C. E., & Fusi Pecci, F. 1985, A&A, 145, 97
- Buonanno, R., Corsi, C. E., Fusi Pecci, F., Alcaino, G., & Liller, W. 1984, A&AS, 57, 75
- Burgarella, D., & Buat, V. 1996, A&A, 313, 129
- Buser, R., & Kurucz, R. L. 1978, A&A, 70, 555
- Buzzoni, A., Fusi Pecci, F., Buonanno, R., & Corsi, C. 1983, A&A, 128, 94

- Byun, Y.-I., & Lee, Y.-W. 1991, in ASP Conf. Ser. Vol. 13, The Formation and Evolution of Star Clusters, ed. K. Janes (San Francisco: ASP), 243
- Cannon, R. D. 1981, in IAU Colloq. 68, Astrophysical Parameters for Globular Clusters, ed. A. G. D. Philip & D. S. Hayes (Schenectady: L. Davis Press), 501
- Caputo, F., Natta, A., & Castellani, V. 1973, *Ap&SS*, 22, 213
- Carney, B., Fullton, L., & Trammell, S. 1991, *AJ*, 101, 1699
- Castellani, M., & Castellani, V. 1993, *ApJ*, 407, 649
- Castellani, V. 1994, *MSAIt*, 65, 149
- Castellani, V., Degl’Innocenti, S., & Pulone, L. 1995, *ApJ*, 446, 228
- Catelan, M. 1993, *A&AS*, 98, 547
- Catelan, M. 1997, *ApJ*, 478, L99
- Catelan, M., & de Freitas Pacheco, J. A. 1993, *AJ*, 106, 175
- Catelan, M., & de Freitas Pacheco, J. A. 1996, *PASP*, 108, 166
- Catelan, M., & de Freitas Pacheco, J. A., & Horvath, J. E. 1996, *ApJ*, 461, 231
- Catelan, M., & Sweigart, A. V. 1997, in preparation
- Clement, C. M. 1996, An Update to Helen Sawyer Hogg’s Third Catalogue of Variable Stars in Globular Clusters, in preparation
- Clement, C. M., & Hazen, M. L. 1989, *AJ*, 97, 414
- Crocker, D. A., Rood, R. T., & O’Connell R. W. 1988, *ApJ*, 332, 236
- Da Costa, G. S., Norris, J., & Willumsen, J. V. 1986, *ApJ*, 308, 743
- D’Cruz, N. L., Dorman, B., Rood, R. T., & O’Connell, R. W. 1996, *ApJ*, 466, 359
- Desidera, S. 1996, Studio delle Stelle Evolute negli Amassi Globulari Galattici, Tesi di Laurea (Padova, Università di Padova)
- Dixon, W. V. D., Davidsen, A. F., Dorman, B., & Ferguson, H. C. 1996, *AJ*, 111, 1936
- Dorman, B. 1997, private communication
- Durrell, P. R., & Harris, W. E. 1993, *AJ*, 105, 1420
- Ferraro, F. R., Carretta, E., Corsi, C. E., Fusi Pecci, F., Cacciari, C., Buonanno, R., Paltrinieri, B., & Hamilton, D. 1997a, *A&A*, 320, 757
- Ferraro, F. R., Clementini, G., Fusi Pecci, F., Buonanno, R., & Alcaïno, G. 1990, *A&AS*, 84, 59
- Ferraro, F. R., Clementini, G., Fusi Pecci, F., Sortino, R., & Buonanno, R. 1992a, *MNRAS*, 256, 391
- Ferraro, F. R., Clementini, G., Fusi Pecci, F., Vitiello, E., & Buonanno, R. 1993, *MNRAS*, 264, 273

- Ferraro, F. R., Fusi Pecci, F., & Buonanno, R. 1992b, MNRAS, 256, 376
- Ferraro, F. R., Fusi Pecci, F., Guarnieri, M. D., Moneti, A., Origlia, L., & Testa, V. 1994, MNRAS, 266, 829
- Ferraro, F. R., Paltrinieri, B., Fusi Pecci, F., Cacciari, C., Dorman, B., & Rood, R. T. 1997b, ApJ, 484, L175
- Ferraro, F. R., & Paresce, F. 1993, AJ, 106, 154
- Fullton, L. K., & Carney, B. W. 1996, in ASP Conf. Ser. Vol. 92, Formation of the Galactic Halo...Inside and Out, ed. H. Morrison & A. Sarajedini (San Francisco: ASP), 265
- Fusi Pecci, F., & Bellazzini, M. 1997, in The Third Conference on Faint Blue Stars, ed. A. G. D. Philip (Schenectady: L. Davis Press), in press
- Fusi Pecci, F., Ferraro, F. R., Bellazzini, M., Djorgovski, S., Piotto, G., & Buonanno, R. 1993, AJ, 105, 1145
- Fusi Pecci, F., Ferraro, F. R., Corsi, C. E., Cacciari, C., & Buonanno, R. 1992, AJ, 104, 1831
- Gratton, R. G., Carretta, E., & Castelli, F. 1996, A&A, 314, 191
- Harris, W. E. 1974, ApJ, 192, L161
- Harris, W. E. 1975, ApJS, 29, 397
- Harris, W. E. 1996, AJ, 112, 1487
- Harris, W. E., Durrell, P. R., Petitpas, G. R., Webb, T. M., & Woodworth, S. C. 1997a, AJ, in press (astro-ph/9707049)
- Harris, W. E., et al. 1997b, AJ, in press (astro-ph/9707048)
- Hawarden, T. G. 1971, Observatory, 91, 78
- Hill, G. 1982, Publ. Dom. Astrophys. Obs., 16, 67
- Hughes, J. A., & Wallerstein, G. 1997, PASP, 109, 274
- Kadla, Z. I., Brocato, E., Piersimoni, A., Gerashchenko, A. N., & Malakhova, Yu. N. 1995, A&A, 302, 723
- Kaluzny, J. 1996, A&AS, 120, 83
- Kaluzny, J. 1997, A&AS, 122, 1
- Kaluzny, J., Kubiak, M., Szymański, M., Udalski, A., Krzemiński, W., & Mateo, M. 1996, A&AS, 120, 139
- Kaluzny, J., Kubiak, M., Szymański, M., Udalski, A., Krzemiński, W., Mateo, M., & Stanek, K. 1997, A&AS, 122, 471
- Koopmann, R. A., Lee, Y.-W., Demarque, P., & Howard, J. M. 1994, ApJ, 423, 380
- Kurucz, R. L. 1992, in IAU Symp. 149, The Stellar Populations of Galaxies, ed. B. Barbuy & A. Renzini (Dordrecht: Kluwer), 225

- Landsman, W. B. 1994, in *Hot Stars in the Galactic Halo*, ed. S. J. Adelman, A. R. Upgren, & C. J. Adelman (Cambridge: Cambridge University Press), 156
- Lee, Y.-W., & Demarque, P. 1990, *ApJS*, 73, 709
- Lee, Y.-W., Demarque, P., & Zinn, R. 1988, in *IAU Symp. 126, Globular Cluster Systems in Galaxies*, ed. J. E. Grindlay & A. G. D. Philip (Dordrecht: Kluwer), 505
- Lee, Y.-W., Demarque, P., & Zinn, R. 1994, *ApJ*, 423, 248
- Lejeune, Th., Cuisinier, F., & Buser, R. 1997, *A&A*, in press (astro-ph/9701019)
- Markov, H. 1997, private communication
- Mironov, A. V. 1972, *AZh*, 49, 134
- Montgomery, K. A. 1995, *Old Stellar Systems: A Study in Stellar and Galactic Evolution*, PhD Thesis (Boston: Boston University)
- Mould, J. R., et al. 1996, *ApJ*, 461, 762
- Newell, E. B. 1970, *ApJ*, 159, 443
- Newell, E. B. 1973, *ApJS*, 26, 37
- Newell, E. B., & Sadler, E. M. 1978, *ApJ*, 221, 825
- Newman, W. I., Haynes, M. P., & Terzian, Y. 1989, *ApJ*, 344, 111
- Norris, J. 1981, *ApJ*, 248, 177
- Norris, J., Cottrell, P. L., Freeman, K. C., & Da Costa, G. S. 1981, *ApJ*, 244, 205
- Parise, R. A., et al. 1994, *ApJ*, 423, 305
- Piotto, G., et al. 1997, in *Advances in Stellar Evolution*, ed. R. T. Rood & A. Renzini (Cambridge: Cambridge University Press), 84
- Racine, R. 1971, *AJ*, 76, 331
- Reid, N. 1996, *MNRAS*, 278, 367
- Renzini, A., & Fusi Pecci, F. 1988, *ARA&A*, 26, 199
- Rich, R. M., et al. 1997, *ApJ*, 484, L25
- Rood, R. T., & Crocker, D. A. 1985a, in *ESO Workshop on Production and Distribution of C, N, O Elements* (Garching: ESO), 61
- Rood, R. T., & Crocker, D. A. 1985b, in *Horizontal-Branch and UV-Bright Stars*, ed. A. G. D. Philip (Schenectady: L. Davis Press), 99
- Rood, R. T., & Crocker, D. A. 1989, in *IAU Colloq. 111, The Use of Pulsating Stars in Fundamental Problems of Astronomy*, ed. E. G. Schmidt (Cambridge: Cambridge University Press), 103

- Rood, R. T., Crocker, D. A., Fusi Pecci, F., Ferraro, F. R., Clementini, G., & Buonanno, R. 1993, in ASP Conf. Ser. Vol. 48, *The Globular Cluster–Galaxy Connection*, ed. G. H. Smith & J. P. Brodie (San Francisco: ASP), 218
- Salaris, M., Chieffi, A., & Straniero, O. 1993, *ApJ*, 414, 580
- Samus, N., Kravtsov, V., Pavlov, M., Alcaíno, G., & Liller, W. 1995, *A&AS*, 109, 487
- Sandage, A., Katem, B., & Kristian, J. 1968, *ApJ*, 153, L129
- Sandage, A., & Smith, L. L. 1966, *ApJ*, 144, 886
- Sandquist, E. L., Bolte, M., Stetson, P. B., & Hesser, J. E. 1996, *ApJ*, 470, 910
- Sarajedini, A. 1992, *AJ*, 104, 178
- Saviane, I., Piotto, G., Fagotto, F., Zaggia, S., Capaccioli, M., & Aparicio, A. 1997, *A&A*, in press
- Sawyer Hogg, H. 1973, *Publ. David Dunlap Obs.*, 3, No. 6
- Shi, X. 1995, *ApJ*, 446, 637
- Silbermann, N. A., & Smith, H. A. 1996, *AJ*, 111, 567
- Smith, H. A., & Stryker, L. L. 1986, *PASP*, 98, 453
- Smith, G. H., & Norris, J. 1983, *ApJ*, 264, 215
- Sosin, C., et al. 1997a, *ApJ*, 480, L35
- Sosin, C., Piotto, G., Djorgovski, S., King, I. R., Rich, R. M., Dorman, B., Liebert, J., & Renzini, A., & 1997b, in *Advances in Stellar Evolution*, ed. R. T. Rood & A. Renzini (Cambridge: Cambridge University Press), 92
- Stetson, P. B. 1981, *AJ*, 86, 687
- Stetson, P. B., VandenBerg, D. A., & Bolte, M. 1996, *PASP*, 108, 560
- Sweigart, A. V. 1987, *ApJS*, 65, 95
- Sweigart, A. V. 1994, *ApJ*, 426, 612
- Sweigart, A. V. 1997a, *ApJ*, 474, L23
- Sweigart, A. V. 1997b, in *The Third Conference on Faint Blue Stars*, ed. A. G. D. Philip (Schenectady: L. Davis Press), in press
- Sweigart, A. V., & Catelan, M. 1997a, in *A Half Century of Stellar Pulsation Interpretations: A Tribute to Arthur N. Cox* (San Francisco: ASP), in press
- Sweigart, A. V., & Catelan, M. 1997b, *ApJ*, in preparation
- Sweigart, A. V., & Gross, P. G. 1976, *ApJS*, 32, 367
- Sweigart, A. V., & Gross, P. G. 1978, *ApJS*, 36, 405
- van den Bergh, S. 1996, *ApJ*, 471, L31
- Walker, A. 1992, *PASP*, 104, 1063

Walker, A. 1994, *AJ*, 108, 555

Walker, A. R., & Nemec, J. M. 1996, *AJ*, 112, 2026

Watson, A. M., et al. 1994, *ApJ*, 435, L55

Whitney, J. H., et al. 1994, *AJ*, 108, 1350

Wichmann, B., & Hill, D. 1987, *Byte*, March, 127

Yanny, B., Guhathakurta, P., Schneider, D. P., & Bahcall, J. N. 1994, *ApJ*, 435, L59

Yi, S., Lee, Y.-W., & Demarque, P. 1995, *ApJ*, 411, L25

TABLE 1
OBSERVED VS. SIMULATED HB MORPHOLOGY PARAMETERS FOR NGC 6229.^a

	$\frac{B}{B+R}$	$\frac{B-R}{B+V+R}$	$\frac{B^2-R}{B+V+R}$	$B : V : R$	L_t	HB_{RE}
Observed	0.63	0.24	0.080	0.570 : 0.097 : 0.333	14.1	0.70
Model, UMD	0.65 (0.03)	0.28 (0.06)	0.097 (0.058)	0.592 : 0.094 : 0.314 (0.033) (0.020) (0.031)	13.7 (0.5)	0.73 (0.02)
Model, BMD	0.64 (0.02)	0.25 (0.03)	0.075 (0.032)	0.576 : 0.099 : 0.325 (0.016) (0.019) (0.020)	13.4 (0.6)	0.70 (0.02)

^a Values in parentheses represent the standard deviation of the mean for a sample with $N = 1,000$ simulations.

TABLE 2
MODEL HB MORPHOLOGY PARAMETERS FOR NGC 6229, IN THE LIMIT $\Delta V_{lim}^{RR} \rightarrow \infty$.

	$\frac{B}{B+R}$	$\frac{B-R}{B+V+R}$	$\frac{B^2-R}{B+V+R}$	$B : V : R$	L_t	HB_{RE}
UMD	0.74	0.45	0.31	0.69 : 0.07 : 0.24	17.5	0.70
BMD	0.64	0.24	0.08	0.57 : 0.10 : 0.33	14.8	0.70

TABLE 3
OBSERVED VS. MODEL (UMD) HB MORPHOLOGY PARAMETERS FOR NGC 1851.^a

	$\frac{B}{B+R}$	$\frac{B-R}{B+V+R}$	$\frac{B^2-R}{B+V+R}$	$B : V : R$	L_t	HB_{RE}
Observed	0.34	-0.29	-0.43	0.30 : 0.10 : 0.60	10	0.73
Model, UMD	0.34 (0.04)	-0.28 (0.07)	-0.43 (0.05)	0.296 : 0.127 : 0.577 (0.033) (0.024) (0.037)	14.6 (1.3)	0.73 (0.02)

^a Values in parentheses represent the standard deviation of the mean for a sample with $N = 100$ simulations.

TABLE 4
BIMODAL-HB GLOBULAR CLUSTERS (SEE TEXT).

Cluster (NGC)	Other	[Fe/H]	c	Reference
NGC 1851		-1.26	2.24	Stetson (1981) Walker (1992) Saviane et al. (1997)
NGC 2808		-1.37	1.77	Harris (1974) Ferraro et al. (1990) Sosin et al. (1997a)
NGC 6121	M4	-1.20	1.59	Norris (1981) Lee et al. (1988) Paper I
NGC 6229		-1.44	1.61	Paper I
NGC 6362		-1.06	1.10	Paper I
NGC 6388		-0.60	1.70	Rich et al. (1997)
NGC 6441		-0.53	1.85	Rich et al. (1997)
NGC 6712		-1.01	0.90	Caputo, Natta, & Castellani (1973) Menzies (1974)
NGC 6723		-1.12	1.05	Menzies (1974) Lee et al. (1988) Paper I
NGC 6864	M75	-1.32	1.88	Paper I
	Palomar 2	-1.30	1.45	This paper

TABLE 5
“GAP” GLOBULAR CLUSTERS (SEE TEXT).

Cluster (NGC)	Other	[Fe/H]	c	Reference
NGC 288		-1.24	0.96	Buonanno et al. (1984) Crocker et al. (1988) Bergbusch (1993)
NGC 2419		-2.12	1.40	Harris et al. (1997b)
NGC 2808		-1.37	1.77	Sosin et al. (1997a)
NGC 4590	M68	-2.06	1.64	Walker (1994)
NGC 5139	ω Cen	-1.62	1.24	Da Costa, Norris, & Willumsen (1986) Bailyn et al. (1992) Whitney et al. (1994) Kaluzny et al. (1996, 1997)
NGC 6205	M13	-1.54	1.49	Newell (1970) Racine (1971) Newell & Sadler (1978) Ferraro et al. (1997b)
NGC 6229		-1.44	1.61	Carney et al. (1991) Paper I
NGC 6341	M92	-2.29	1.81	Buonanno et al. (1985) Crocker et al. (1988)
NGC 6388		-0.60	1.70	Piotto et al. (1997)
NGC 6441		-0.53	1.85	Piotto et al. (1997)
NGC 6638		-0.99	1.40	Smith & Stryker (1986)
NGC 6681	M70	-1.51	Core-Collapsed	This paper
NGC 6752		-1.55	Core-Collapsed	Newell & Sadler (1978) Cannon (1981) Buonanno et al. (1986) Crocker et al. (1988)
NGC 6809	M55	-1.81	0.76	Desidera (1996)
NGC 7078	M15	-2.22	Core-Collapsed	Battistini et al. (1985) Buonanno et al. (1985) Crocker et al. (1988) Durrell & Harris (1993) Ferraro & Paresce (1993) Hughes & Wallerstein (1997)
	IC 4499	-1.60	1.11	Walker & Nemeč (1996)

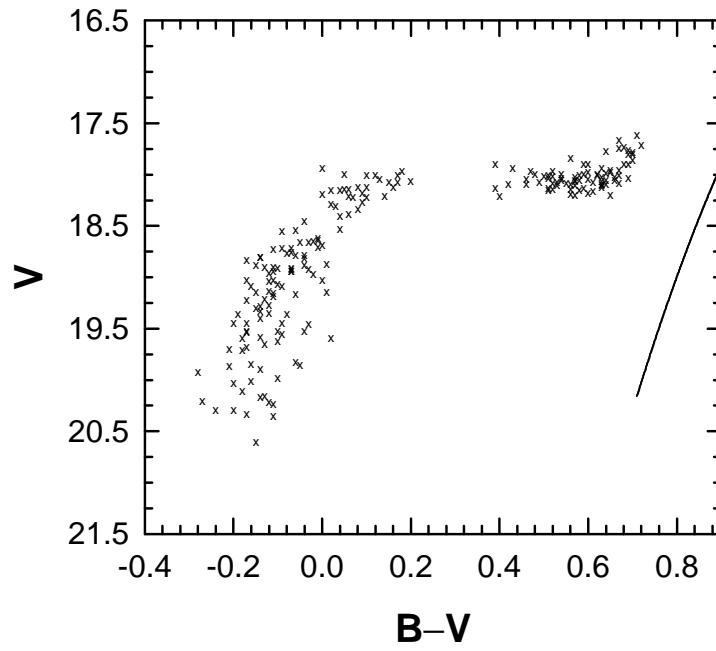


Fig. 1.— The HB region of the NGC 6229 CMD from Paper I. RR Lyrae variables have not been plotted. The position of the RGB is schematically indicated as a solid line.

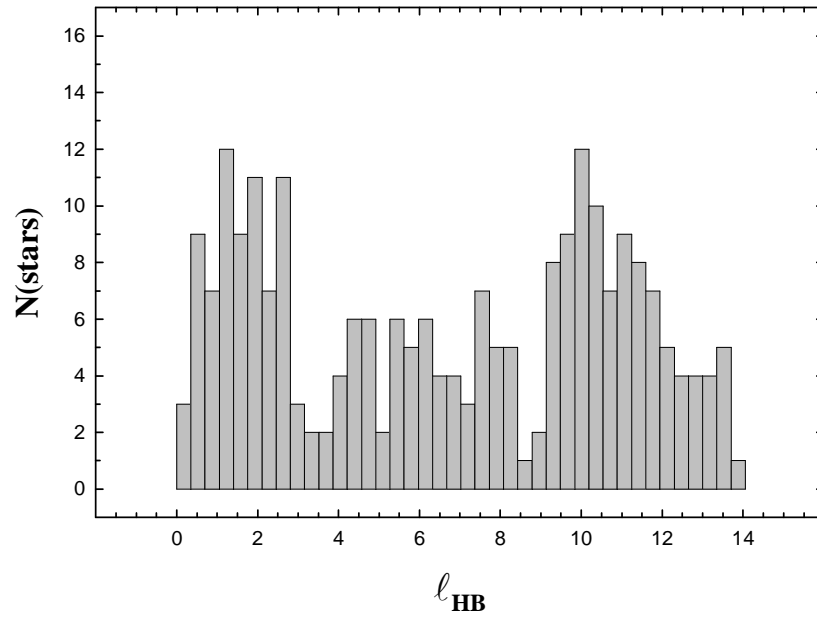


Fig. 2.— l_{HB} distribution for NGC 6229 from the data in Fig. 1. A total of 31 RR Lyrae stars was included with randomly distributed colors inside the instability strip.

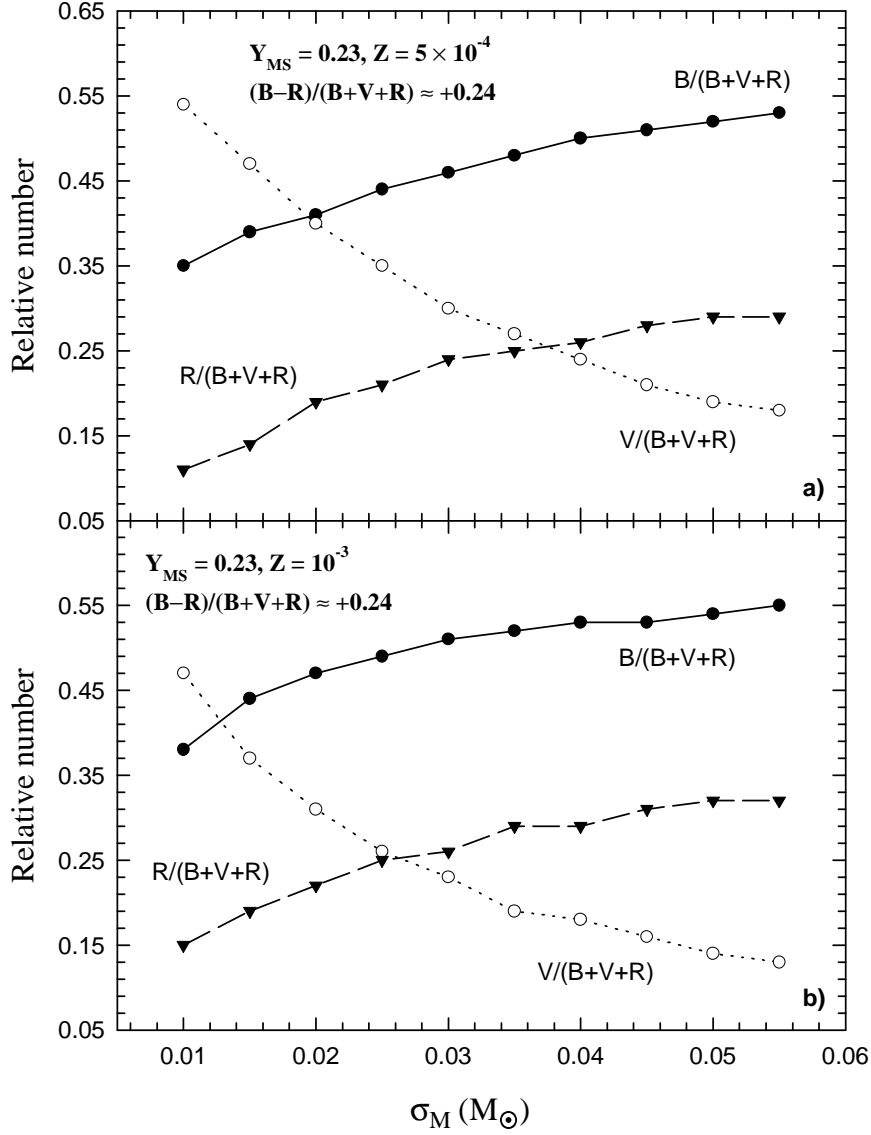


Fig. 3.— The variation of $V/(B + V + R)$ as a function of the HB mass dispersion σ_M as compared with the corresponding variations in $B/(B + V + R)$ and $R/(B + V + R)$ for two metallicities, $Z = 0.0005$ (panel a) and $Z = 0.001$ (panel b). The Lee-Zinn parameter $(B - R)/(B + V + R)$ was held fixed at the value appropriate for NGC 6229.

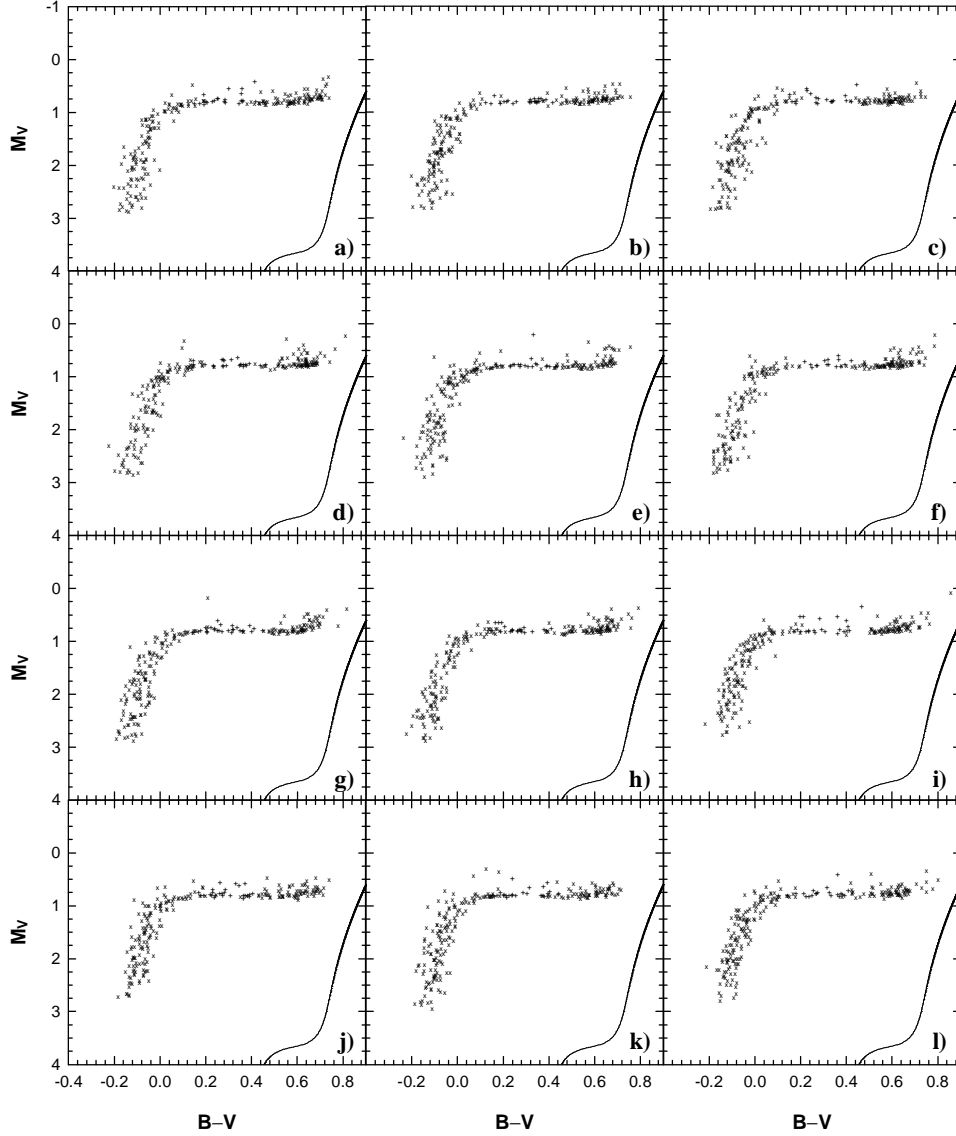


Fig. 4.— Random sample of 12 HB simulations for NGC 6229, obtained from the set of 1,000 synthetic HBs computed for the unimodal mass distribution case discussed in Sec. 4. RR Lyrae variables are indicated by plus signs. The solid lines show the position of an RGB evolutionary track with $M = 0.820 M_{\odot}$.

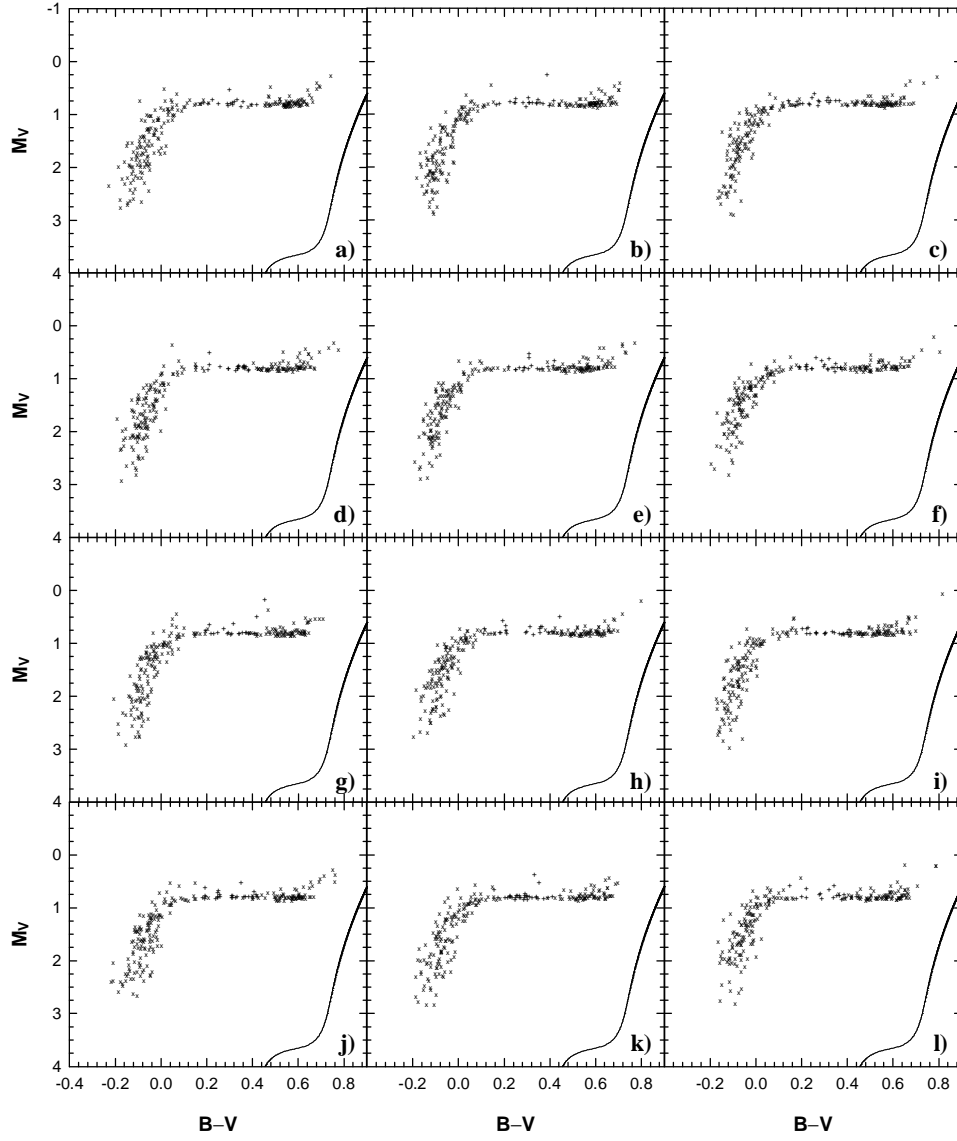


Fig. 5.— As in Fig. 4, but for the bimodal mass distribution case discussed in Sec. 4.

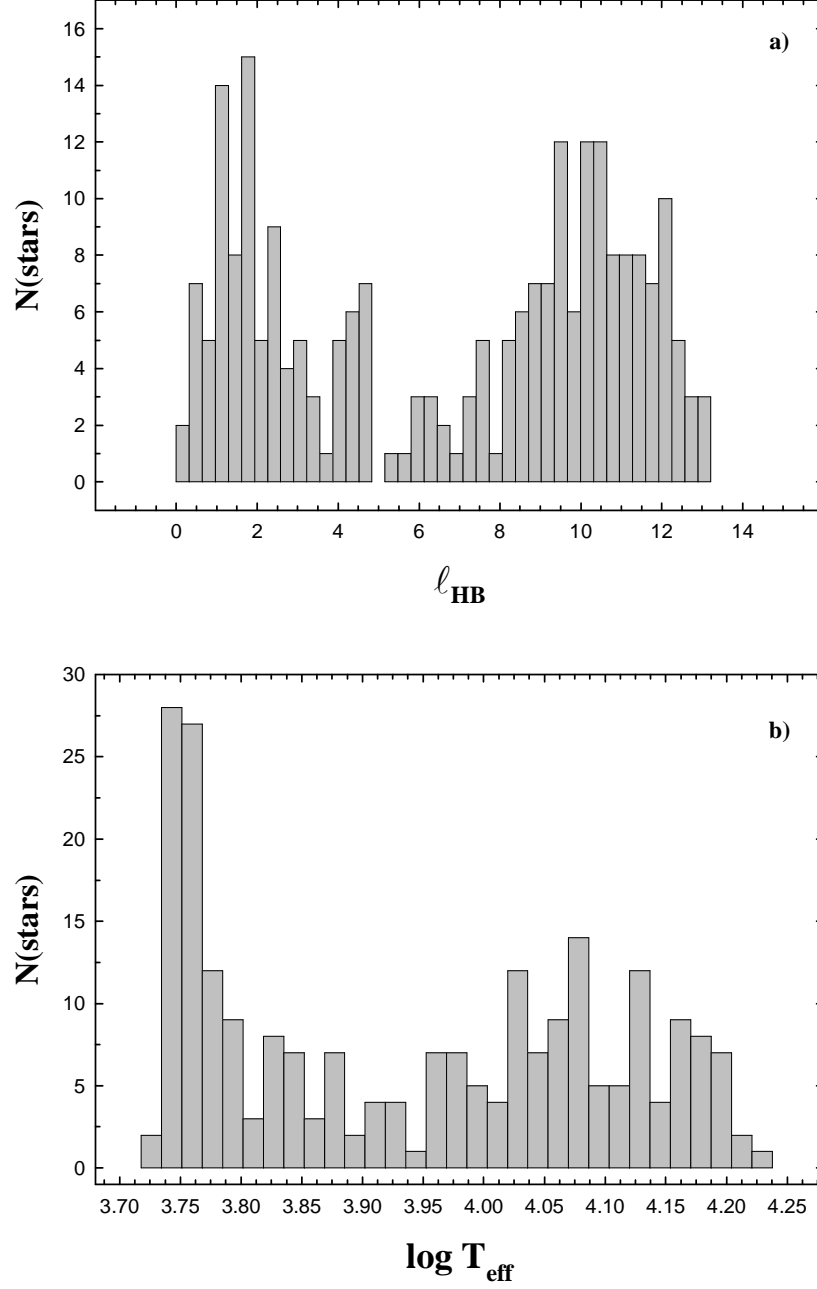


Fig. 6.— Histograms showing the l_{HB} (panel a) and $\log T_{\text{eff}}$ (panel b) distribution for the HB simulation (unimodal mass distribution) displayed in Fig. 4b.

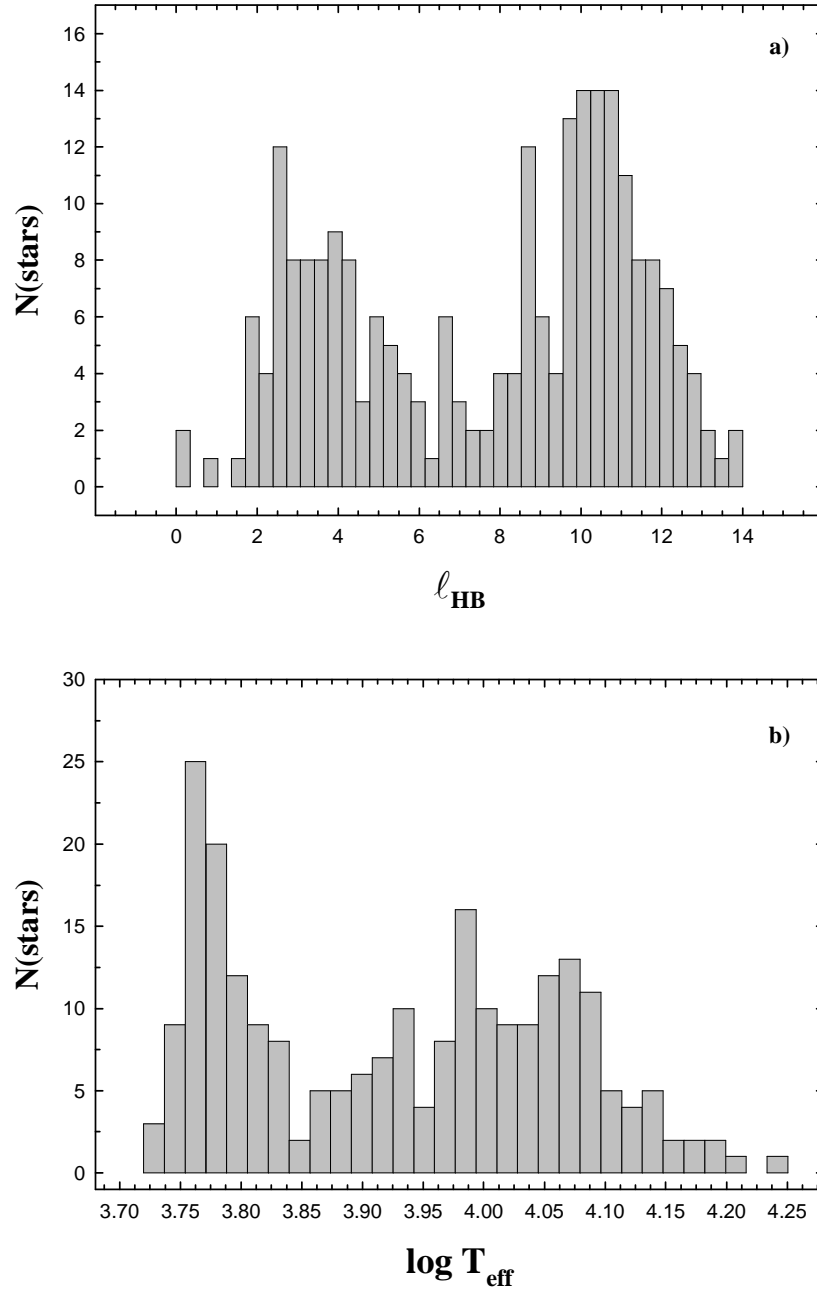


Fig. 7.— As in Fig. 6, but for the HB simulation (bimodal mass distribution) displayed in Fig. 5f.

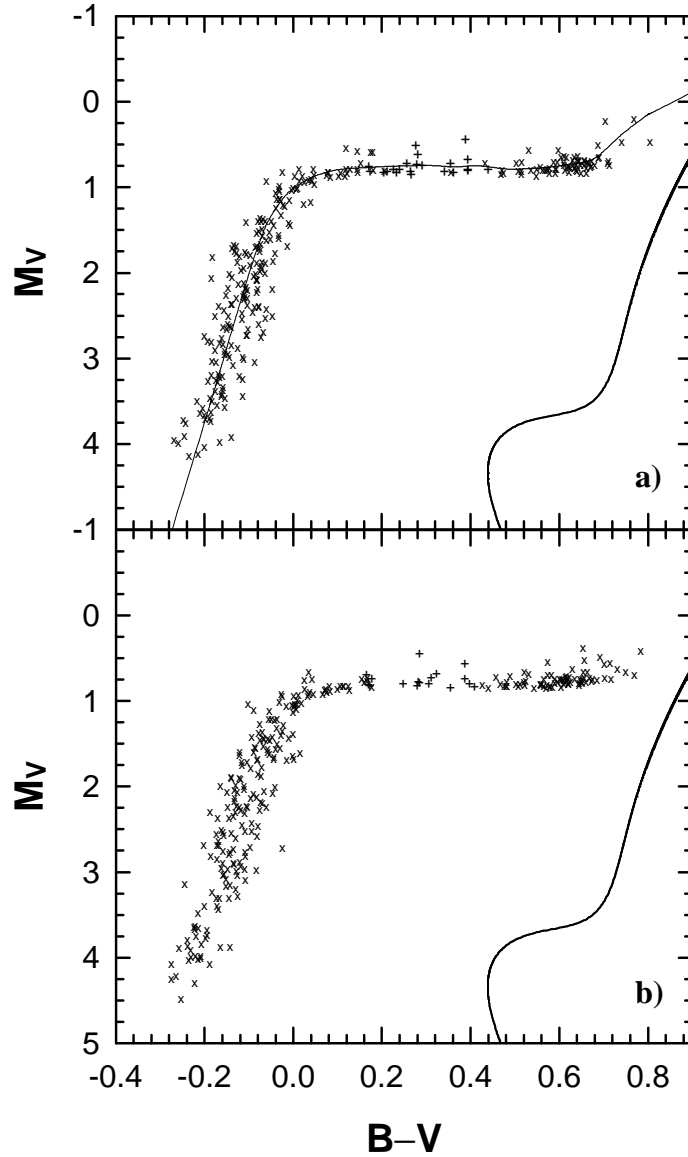


Fig. 8.— Two HB simulations for the same unimodal mass distribution employed in generating Fig. 4, but without truncating the distribution at the faint limit. The computed HB ridgeline is shown as a thin solid line in panel a), and the RGB locus for a $M = 0.820 M_\odot$ star is given as a thick solid line in both panels.

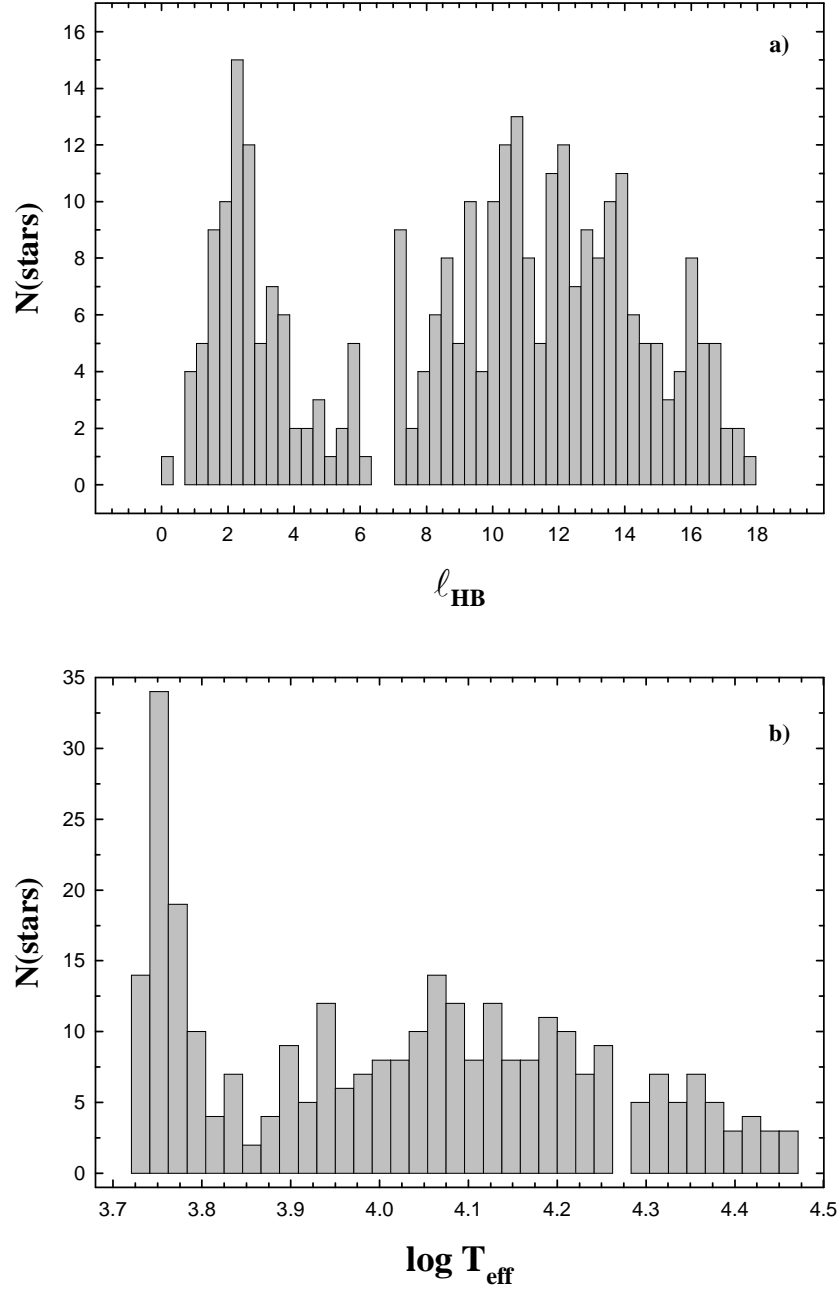


Fig. 9.— Histograms showing the l_{HB} (panel a) and $\log T_{\text{eff}}$ (panel b) distributions for the HB simulation displayed in Fig. 8b.

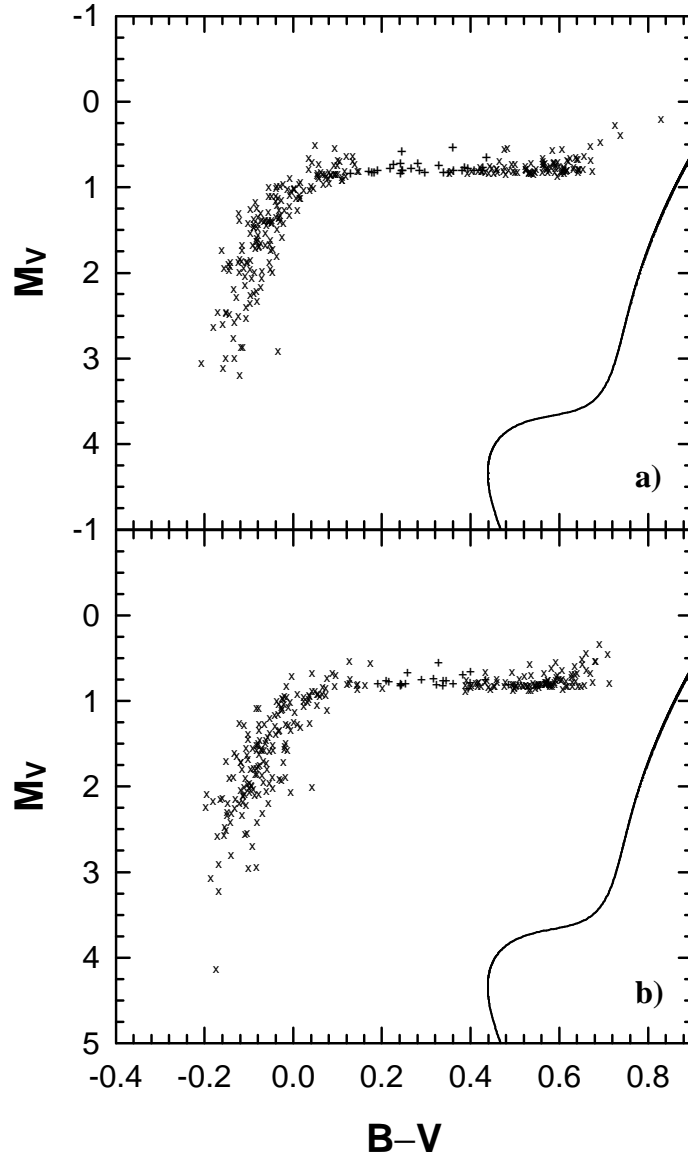


Fig. 10.— Same as Fig. 8, but for a bimodal mass distribution.

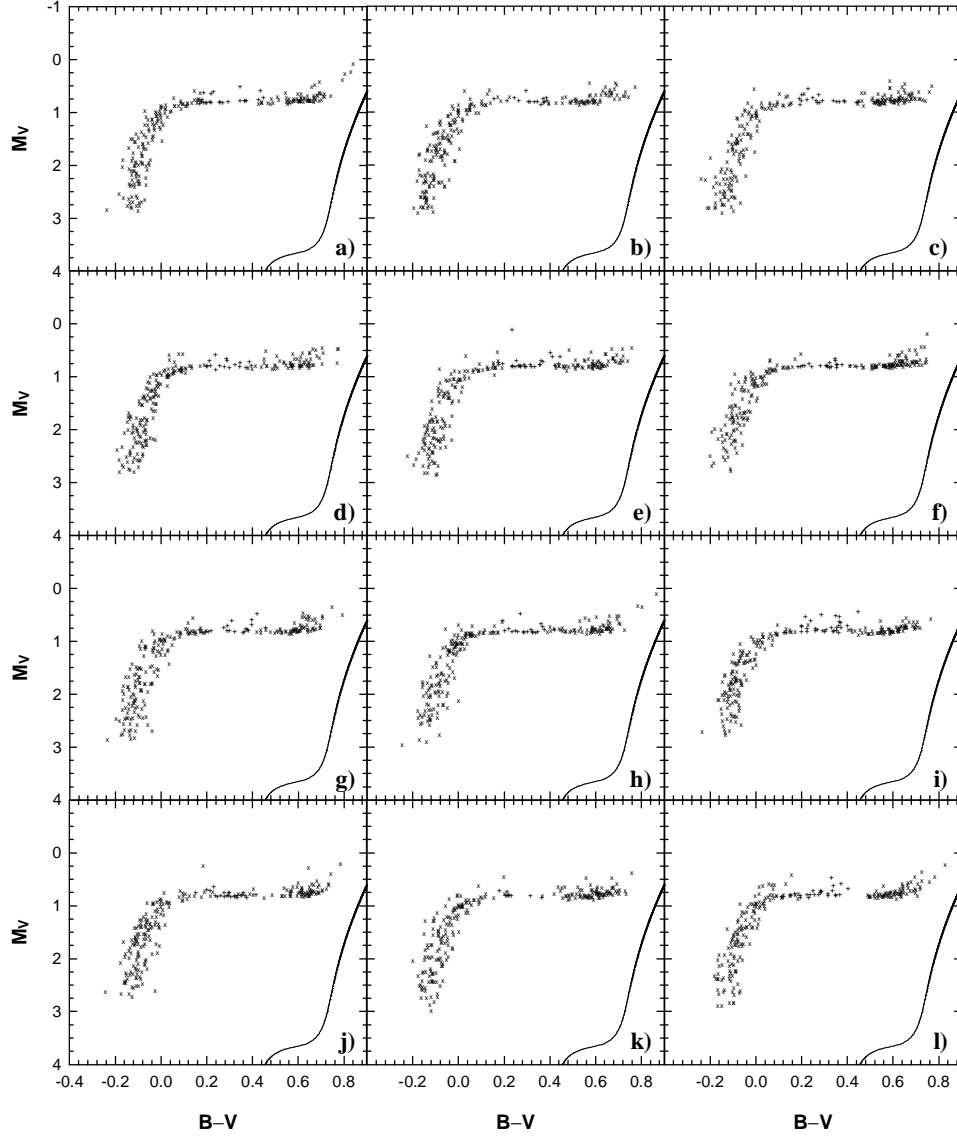


Fig. 11.— Same as Fig. 4, but for a sequence of synthetic HBs showing pronounced gaps at increasingly redder colors [going from a) to l)].

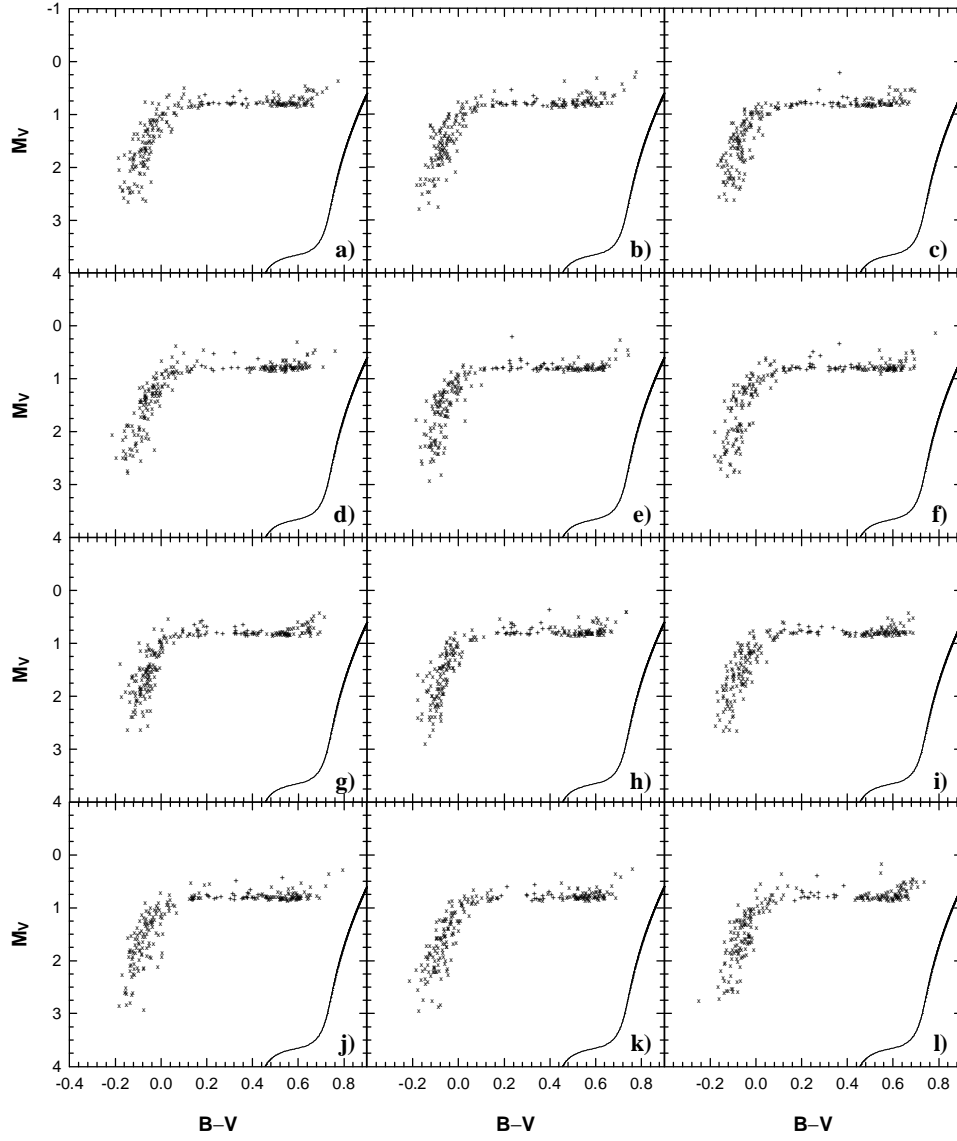


Fig. 12.— Same as Fig. 11, but for a bimodal mass distribution.

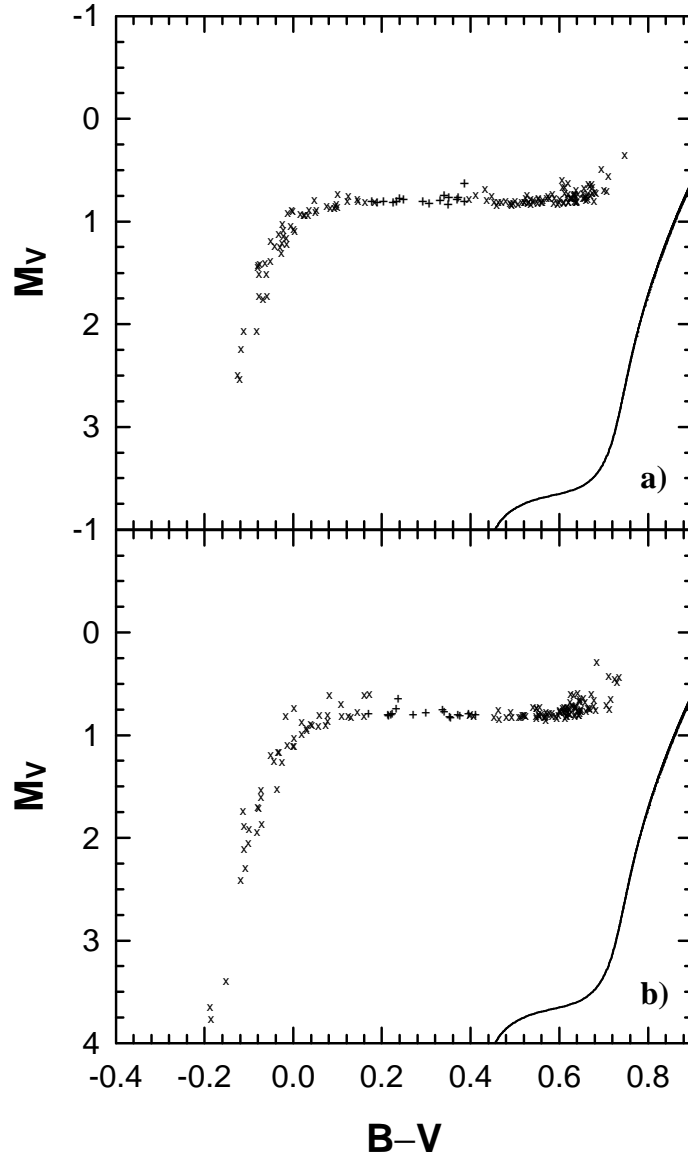


Fig. 13.— Examples of synthetic HBs for NGC 1851.

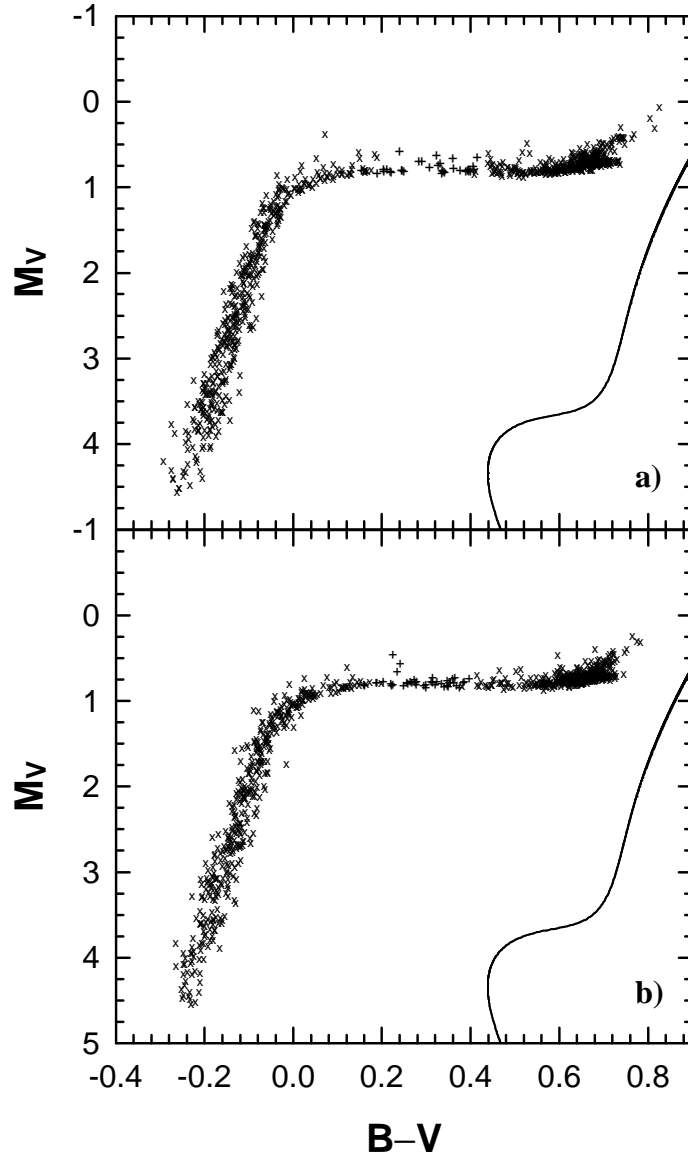
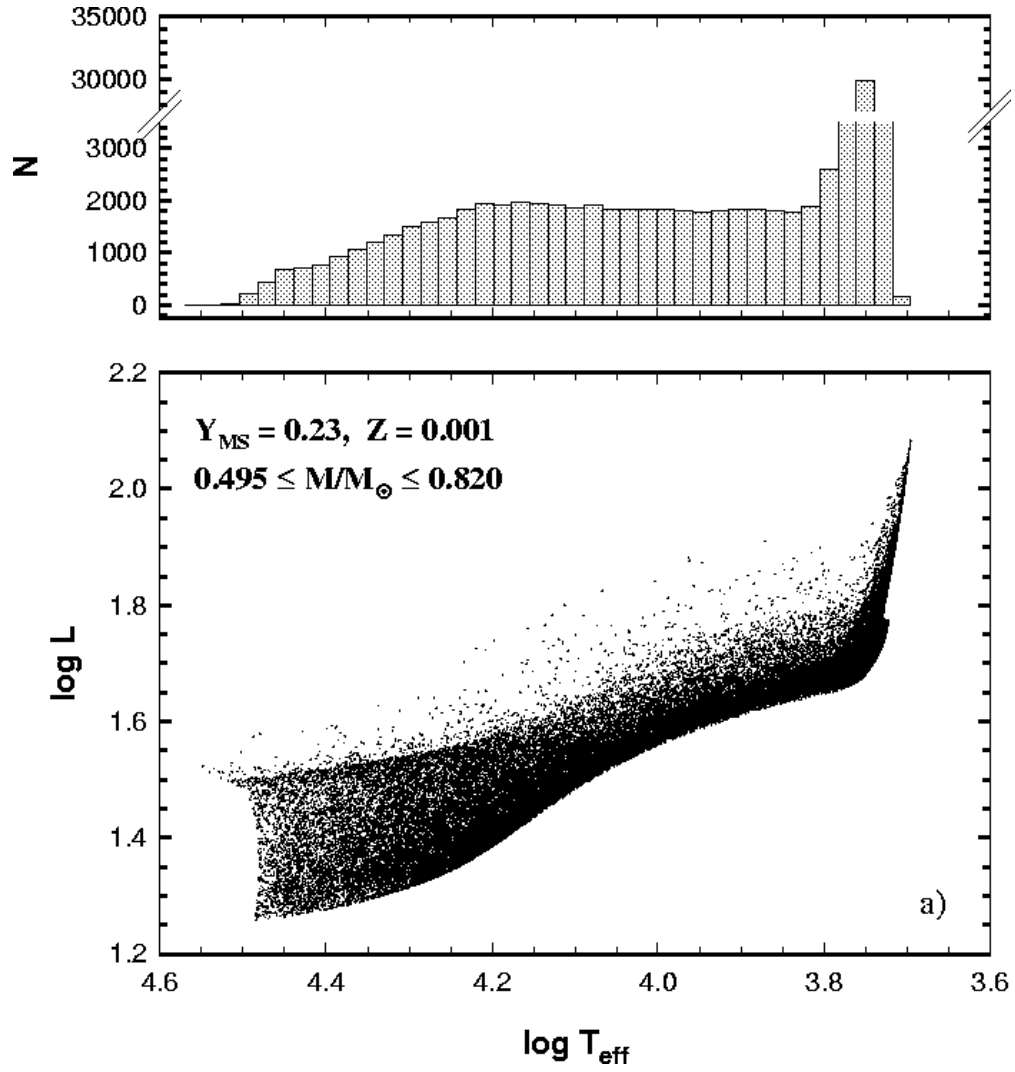


Fig. 14.— Examples of synthetic HBs with a unimodal mass distribution for NGC 2808. These simulations fail to provide a satisfactory match to the observed CMD.



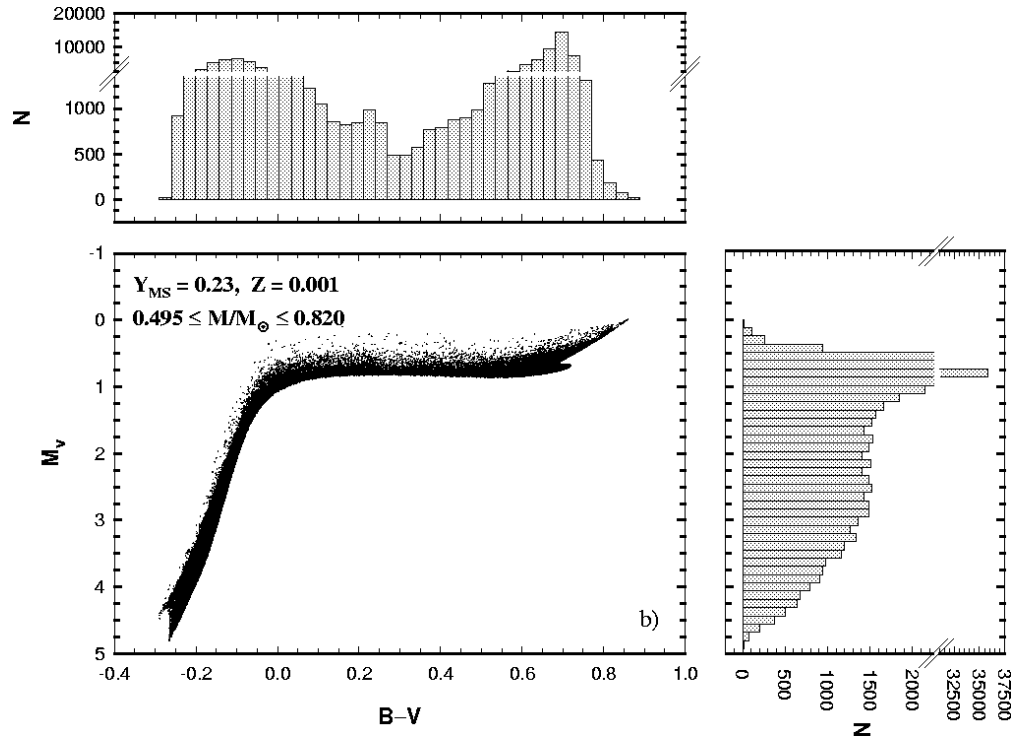


Fig. 15.— Reference synthetic HB simulation with 100,000 stars, computed for a uniform ZAHB mass distribution in the indicated mass range. Panel a) shows the distribution in the $(\log L, \log T_{\text{eff}})$ plane, and panel b) the distribution in the $(M_V, B-V)$ plane. Histograms giving the corresponding distributions in $\log T_{\text{eff}}$, $B-V$, and M_V are also given.

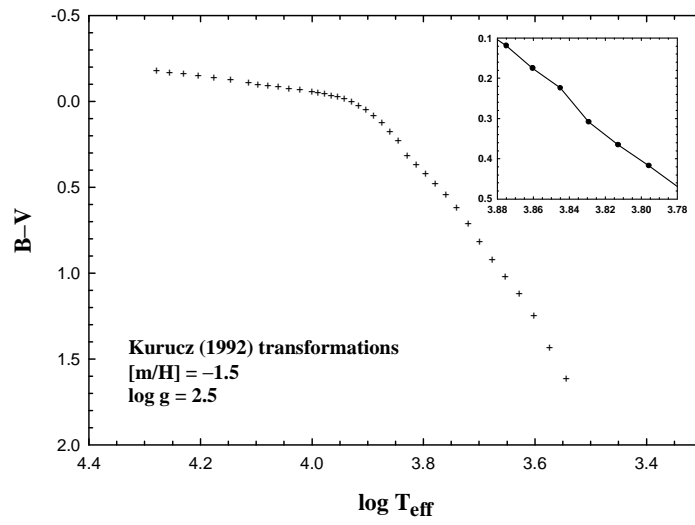


Fig. 16.— Color–temperature relation from the Kurucz (1992) model atmospheres, for the gravity and metallicity values shown on the lower left-hand corner.

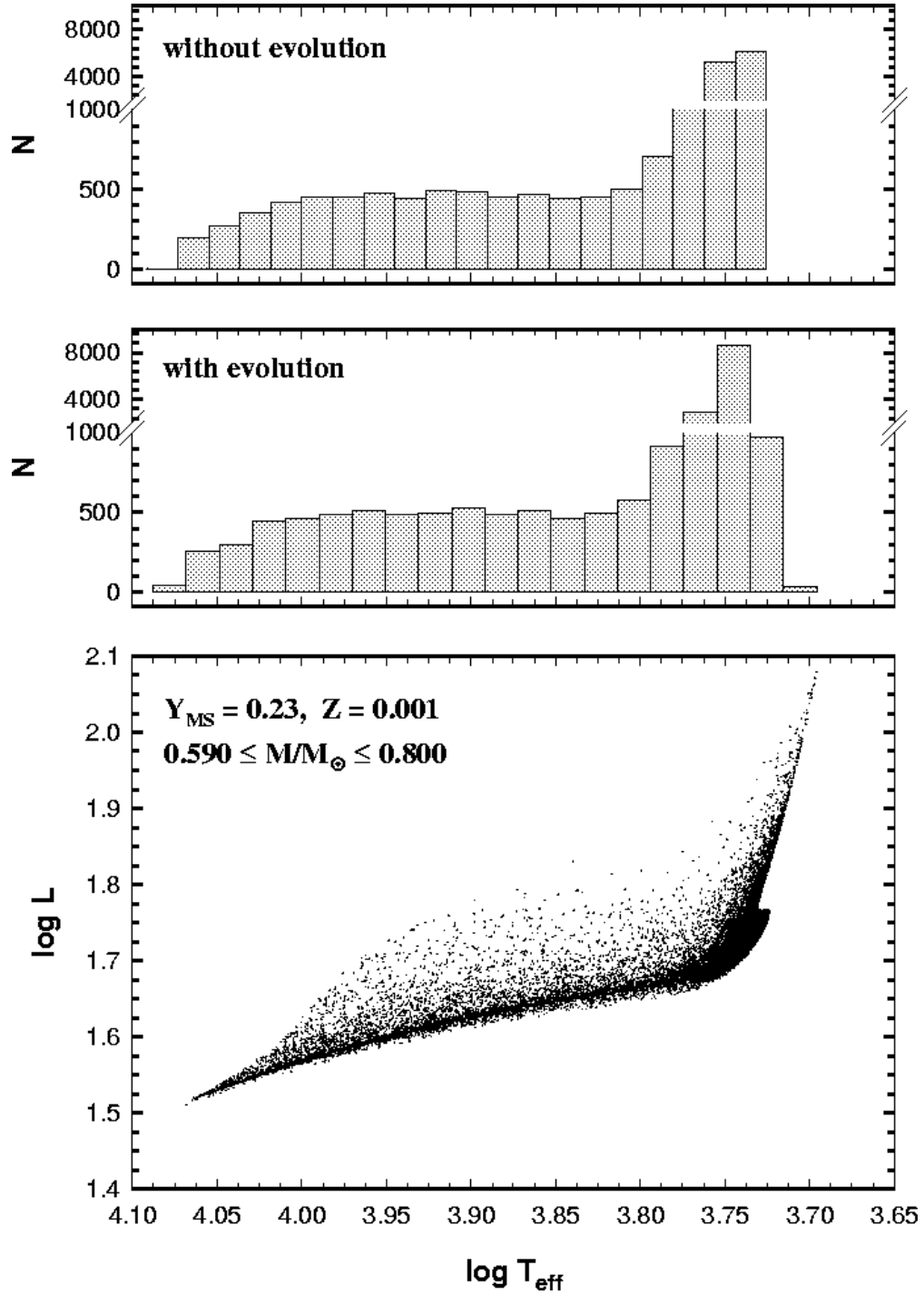


Fig. 17.— A synthetic HB with 20,000 stars, computed for a uniform ZAHB mass distribution in the indicated mass range, is shown in the $(\log L, \log T_{\text{eff}})$ plane (bottom panel). The mass range was chosen so as to mimic Walker’s (1992) Fig. 8 as closely as possible. Histograms for T_{eff} are given both for the case which includes evolution away from the ZAHB (middle panel) and the case where evolution away from the ZAHB is suppressed (upper panel).

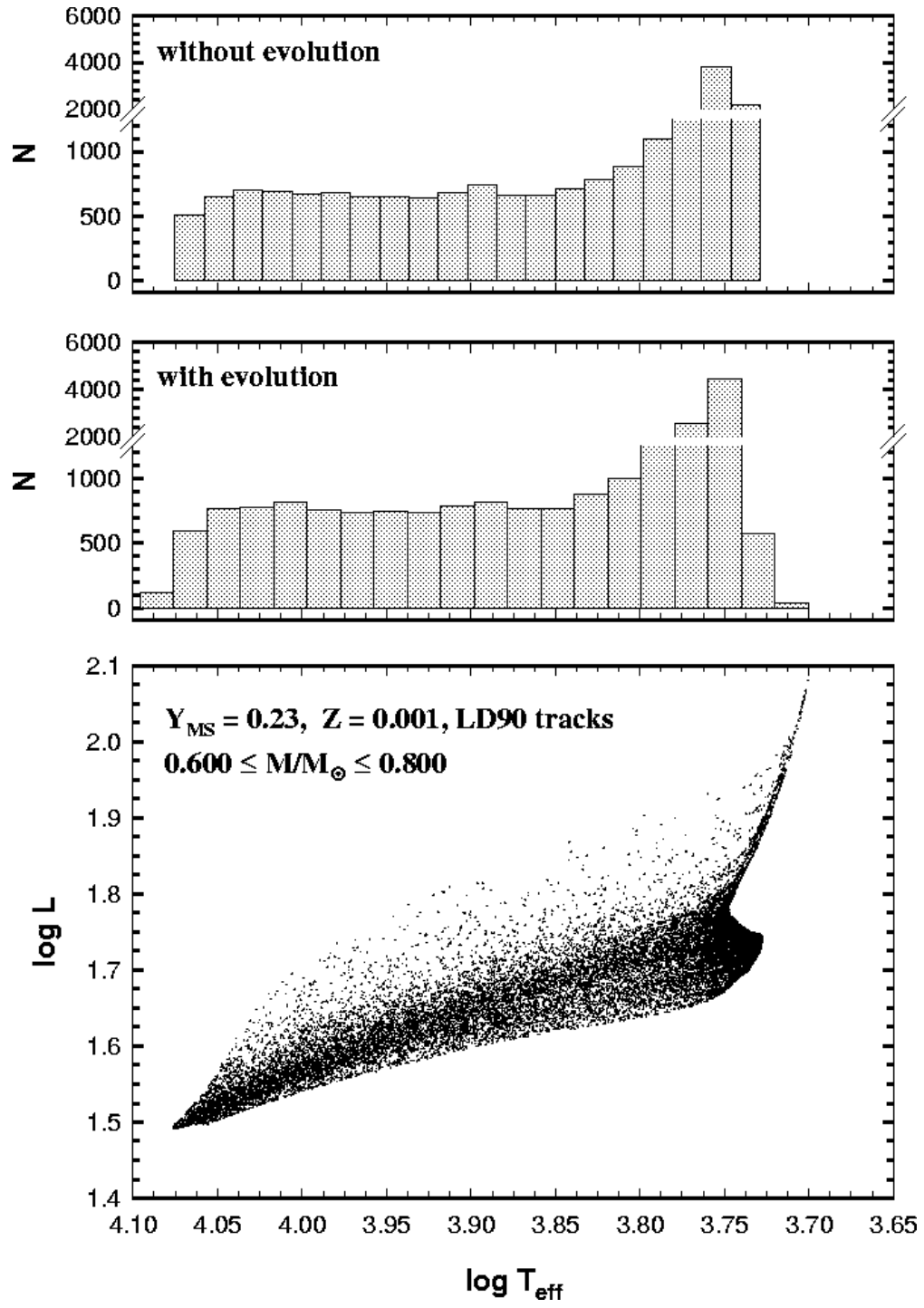


Fig. 18.— As in Fig. 17, but using the Lee & Demarque (1990, LD90) evolutionary tracks.